Heliyon 9 (2023) e19650

Contents lists available at ScienceDirect

Heliyon

journal homepage: www.cell.com/heliyon

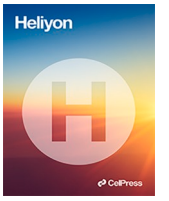

Nonlinear frequency analysis of porous Bi directional functionally graded beams utilizing reddy shear deformation theory

Mohammadamin Forghani [a], Yousef Bazarganlari [a,*], Parham Zahedinejad [b], Mohammad Javad Kazemzadeh-Parsi [a]

[a] Department of Mechanical Engineering, Shiraz Branch Islamic Azad University, Shiraz, Iran
[b] Department of Mechanical and Energy Engineering, North Texas University, NX, USA

ARTICLE INFO

Keywords:
Nonlinear frequency analysis
Bi-directional functionally graded beam
Porous
GDQM
Reddy third-order shear deformation theory

ABSTRACT

The nonlinear frequency response of bi-directional functionally graded porous beams experienced range of various end conditions is investigated in this work. The end conditions which are simply supported, clamped-simply supported, clamped-clamped, and clamped-free are taken by using the Von Karman geometric nonlinearity, Green's tensor and Reddy third-order shear deformation theory. A generalized differential quadrature technique (GDQM) accompanied by direct numerical iterance approach is proposed to solve equations. The findings are presented to aid in future research into the effects of various gradient indices, vibration amplitude ratios, porosity coefficients, shear and elastic substrate parameters, boundary conditions, and vibration frequencies on the bi-directional functionally graded beams. The outcomes of this research have practical applications and can be utilized to enhance the design of bi-directional beams. The results are also highly useful in anticipating and identifying potential causes of failure in these beams.

1. Introduction

Ceramics and metal are the two main components of functionally graded materials. Ceramics is a structural material that can endure high heat since It resists high temperatures and has a low heat transfer constant. Metal, a different structural material, contrasted with, offers the necessary flexibility. Notably, Functionally Graded Materials (FGMs) do not experience the discontinuity issues that are present in typical composite constructions due to the continual modifications in mechanical characteristics. FGMs are superior to traditional composite laminates in several ways, including reduced thermal tensions, low-stress concentrations, attenuated stress waves, etc. FGMs have therefore found extensive use as structural elements in contemporary sectors including mechanical, nuclear, and aerospace engineering. When creating structural elements, FGMs are employed in place of isotropic materials. There is a broad tendency toward vibration analysis of these components under various realistic operating and boundary conditions. Free and forced vibration have been two areas of a study done to date by using various beam theories. Some of them were following classical beam theory (CBT) which is suitable for slender FG beams. Due to overstating the frequencies and omitting the transverse shear deformation impact, the CBT is not relevant for deeper ones. Timoshenko beam theory, commonly known as the first-order shear deformation beam theory, addresses the transverse shear deformation influence in order to improve the CBT [1]. To identify the difference between actual and assumed stress levels, a shear correction factor must be applied to the top and bottom surfaces of the FBT [1].

* Corresponding author.
E-mail address: yo.bazargan@iau.ac.ir (Y. Bazarganlari).

https://doi.org/10.1016/j.heliyon.2023.e19650
Received 18 June 2023; Received in revised form 28 August 2023; Accepted 29 August 2023
Available online 3 September 2023

Higher-order shear deformation theories without a shear correction factor can accurately predict the intrinsic frequency, displacement, and stress variants of moderately thick beams. A higher-order shear deformation model was used to investigate the vibrational behavior of FG beams. Using a higher-order finite element technique, Wen and Zeng [2] studied the frequency analysis of beams. Free vibration of FG beams was examined by Aydogdu and Taskin [3]. A variety of higher-order theories were used by Simsek [4] to define the frequency behavior of FG beams in a variety of terminal situations. Based on a variety of higher-order shear deformation theories, Huu-Tai Thai [5] investigated the free frequency analysis and vibration of FG beams. As a result of different boundary condition collocations based on various higher-order shear deformation beam theories, Pradhan and Chakraverty [6] demonstrated the free vibration behavior of FG beams using the Rayleigh-Ritz method. Using the Chebyshev collocation method and third-order shear deformation theory, Wattanasakulpong et al. [7] investigate the natural frequencies of elastically supported FG beams. Wang et al. use the Chebyshev-Ritz method to study the nonlinear bending of a sandwich beam with metal foam and GPLRC face-sheets using a third-order shear deformation theory supported by the von Kármán nonlinearity [8]. Zhang and Wang have recently re-energized a created third-order shear deformation theory in the temperature-dependent thermo-mechanical outputs of porous functionally graded graphene-reinforced composite panels [9].

Mechanical beams are grounded in several engineering applications. There are many types of construction in this area, including rail lines, geotechnical regions, highway walkways, buildings, offshore constructions, towers, and pipelines. Many scientists investigate how beams form on different elastic substrates due to this reason. Vibrations and bending difficulties with elastically supported beams and columns are common in structural engineering and substructure. Due to its mathematical simplicity, the Winkler base is often used to simulate the elastic basis in soil structure difficulties.

As a result, it has been demonstrated that the linear tensile spring model does not accurately represent the behavior of substrate materials in engineering. As a result of Pasternak's framework, a simple physical model close to simple mathematics was established using two parameters with shear interactions. In several studies, elastic substrates have been found to influence free beam vibration. Based on a general solution, Zhou [10] evaluated the frequency of isotropic beams on varying Winkler elastic substrates. A frequency analysis of isotropic beams on variable-parameter elastic substrates has been conducted by Eisenberger [11]. A two-parameter elastic substrate supported by a FG sandwich beam was investigated by Pradhan and Murmu [12]. To conduct the free vibrations and buckling of two-parameter elastic substrates resting on isotropic thick beams, Malekzadeh and Karami [13] utilized a combined differential quadrature and finite element method. Using the notion of least total potential energy, Akbas [14] extracted the governing system and related end conditions for free vibration and bending of functionally graded (FG) beams resting on the Winkler foundation. The Navier-type measure is implemented for static deflections and fundamental frequencies. To discretize the governing equations, Zahedinejad [1] investigated the free frequency evaluation of functionally graded beams on elastic substrates. Using the Euler-Bernoulli-based generalized differential quadrature method (GDQ), Yas et al. [15] investigated the free vibration of FG beams supported by two elastic substrates. A Chebyshev collocation approach was used by Tossapanon and Wattanasakulpong [16] investigate the frequency behavior of functionally graded beams on two elastic substrates. In many current buildings, the material properties of some structural components will vary in multiple directions due to the temperature field and mechanical stress distributed in multiple directions in the working environment. FG materials with multidirectionally changing material properties should therefore be investigated in two- and three-dimensions. All of the preceding research has focused on FG structures, whose material properties vary solely in one orientation. As a result, traditional FG structures fail to meet the stress and temperature dispersion criteria for aeronautical applications in a variety of orientations. Li et al. investigated two-dimensional functionally graded beams [17]. The two-dimensional FG beams were analyzed with the aid of the Euler-Bernoulli beam theory and the generalized differential quadrature measure to estimate the linearized and nonlinearized displacements. Lei et al. [18] present a study of functionally graded bi-directionally defective beams based on third-order shear deformation theory. Based on Timoshenko beam theory, Mesut Simsek [19] investigated the free frequency behavior of bidirectional functionally graded materials, employing the implicit time integration Newmark method to solve the governing differential system. Zhi-hai Wang et al. [20] investigated an analytical solution for varied supports for two-dimensional functionally graded beams using the Euler-Bernoulli theory, as well as stability analyses of bidirectional functionally graded beams supported on elastic substrate Ghorbanpour [21] has investigated the transient stability of bi-directional functionally graded beams under harmonic excitation and a thermal environment. The study by Kazemzaeh-Parsi et al. [22] examines multi-directional functionally graded plates using 3D elasticity solutions.

Due to the progressive shift in volumetric constituent proportions, functionally graded materials have a non-uniform microstructure and continuously properties. Almost all of the material in this device is ceramic on one side, which is heat-resistant, and metal on the other side, which is strong and durable. Functional grade materials combine these two essential features to enhance heat-resistant properties. The constant modification of these materials prevents cracking and scaling, which are common in layered composites. As the material cures, it can develop tiny holes, voids, or pores due to a significant difference in freezing temperatures between the components. Due to technological difficulties [23], FG materials are expected to have porosities and micro-voids. A number of porosities could result from contraction between the compositions of the metal and ceramic phases in FGM, as described by Zhu et al. [24]. There is a wide span of applications in sectors such as civil engineering, automotive, and aerospace for lightweight beams made of delibrately porous materials. A promising option for structures subjected to unstable stresses is to fabricate FGMs from porous materials [25]. Chen et al. [25] studied shear-induced free and forced vibrations of functionally graded porous beams. They employed the Timoshenko beam hypothesis, the Lagrange equation technique, and Ritz trial functions to account for transverse shear strain in the equation of motion. The equation of motion is then solved in the time domain using the Newmark approach. Based on the theories of Euler-Bernoulli and Timoshenko beams, Rjoub [26] used a transfer matrix approach to derive the natural frequency equations for functionally graded porous beams. Navvab Shafiei et al. [27] proposed a Timoshenko theory-based vibration assessment of bi-directional imperfect functionally graded nano/micro beams made of two unique porous materials. Solving the governing

equations under diverse end conditions is achieved using the generalized differential quadrature method (GDQM). Using a higher-order thermomechanical theory and an analytical solution based on Navier-type solutions, Ebrahimi [28] investigated the frequency evaluation of temperature-dependent FGM beams with voids. Two examples of porous beams were evaluated using a higher order shear deformation and Chebyshev collocation approach by Nauttawit Wattanasakulpong et al. [29]. Jian Lei et al. [18] investigated functionally graded imperfect bidirectional beam post-buckling using a novel third-order shear deformation theory. The extended differential quadrature method, the minimum potential energy concept, and von Karman's nonlinear theory are used to formulate and solve nonlinear partial differential equations. The nonlinear vibration of Timoshenko beams with pores was examined by Ebrahimi et al. [30]. The extended differential quadrature approach was used by Khakpour et al. [31] to investigate how functionally graded porous beams vibrate in a temperature environment.

Our daily experience is dominated by nonlinear phenomena (large amplitude), especially dynamic phenomena such as vibrations. In some cases, nonlinear systems exhibit characteristics that linear systems lack. In the workplace, it is often acceptable to assume linear behavior when dealing with nonlinear problems. However, the scientific community has begun to account for the improved accuracy of findings as a consequence of modern technical breakthroughs. Consequently, nonlinear difficulties have become an important subject in engineering, physics, and other disciplines. Bridges, skyscrapers, robotic arms, and other structures can be thought of as flexible beams from an engineering perspective. These structures are also described using nonlinear motion equations because they respond to natural vibrations in a nonlinear manner. There are three distinct ways in which a structure may become nonlinear: physically, geometrically or due to boundary conditions.

Ebrahimi and Zia [30] proposed porous Timoshenko beams based on the nonlinear vibration features of FGM beams and studied how material variation, void volume percentage, slender ratio and mode number affect vibrational response. Using a massless elastic rotating spring, Kitipornchai et al. [32] studied the nonlinear frequency of edge-fractured functionally graded beams whose material characteristics were based on exponential form through the beam thickness. The Ritz methodology is utilized to create the governing eigenvalue equation in order to determine the nonlinear vibration frequencies of cracked FGM beams with different end supports. To solve the equation, the direct iterative technique is used. Malekzadeh and Shojaee [33] investigated the surface and nonlocal effects on the nonlinear free vibration of non-uniform nanobeams using Hamilton's principle and Eringen's nonlocal elasticity theory in the Euler-Bernoulli beam theory (EBT) and Timoshenko beam theory (TBT). Geometric nonlinearity has been modeled using Green's tensor and von Karman's assumptions. Wattanasakulpong and Chaikittiratana [34] used the differential transformation method (DTM) to solve linear and nonlinear vibration issues of elastically end restrained beams. Using the proposed differential quadrature technique to resolve displacements of bi-dimensional functionally graded (FG) beams rooted in Euler-Bernoulli beam theory (GDQM), Li et al. [17] investigated the nonlinear bending of bi-dimensional functionally graded beams. Tianzhi Yanga et al. [35] investigated bi-directional functionally graded nanobeams with exponential thickness and length gradations. The differential quadrature technique (DQM) is used to solve nonlinear problems. Ghayesh [36] discretized the governing equations of axially functionally graded tapering beams (AFG) subjected to external harmonic excitations using the Galkin technique and the third-order shear deformation beam theory. The force and frequency-amplitude diagrams of the AFG system are used to examine gradient index and tapered ratios. Ke Xie et al. [37] performed a nonlinear free vibration analysis on functionally graded beams using a variety of shear deformation theories. In this study, the Ritz method and the Lagrange equation were employed to construct discrete formulations. Songsuwan et al. [38] have investigated the nonlinear frequency of functionally graded-graphene platelet-reinforced composite (FG-GPLRC) beams subjected to various time-dependent stresses. The displacement fields are represented using third-order shear deformation theory, and the geometric nonlinearity is based on the von Kármán assumption. To obtain linear or nonlinear results, the study employs the Gram-Schmidt-Ritz approach with an iterative measure. Nonlinear transient response of sandwich beams possessing functionally graded porouscore under the action of moving load has recently been investigated by Songsuwan and Wattanasakulpong [39]. The governing equation system was developed using third-order shear deformation theory and the von Kármán assumption of geometrical nonlinearity. To achieve convergence in both the time and geometrical domains, the Gram-Schmidt-Ritz approach was used, together with iterative measures based on Newmark's time-integration.

Due to the inherent complexity of the higher-order shear deformation theory [1], powerful numerical measures are demanded to solve constitutive relations for diverse support conditions. In a range of scientific and technological fields, Bellman et al. [40] introduced the differential quadrature method (DQM). Beginning and boundary value problems can be effectively addressed using the DQM. An overview of the totally improvement of the DQ methodology can be found in Bert and Malik's [41]. The differential quadrature method, with its global domain, is believed to be more effective for nonlinear problems than conventional numerical methods, in particular finite elements and finite differences [42].

Based on Reddy third-order shear deformation theory (RBT), no study has been conducted on the nonlinear frequency of bi-directional FG porous beams. Bi-directional FG porous beams lying on elastic substrates have not been studied for nonlinear frequency assessment. Based on the mid-plane bending and shear variants of the FG beam, a new notation for bi-directional FG beam analysis considers the transverse shear deformation. We study how porosity indexes, aspect ratios, power gradient indexces, and elastic substrate properties affect frequency behavior for a variety of end conditions. In order to calculate the large amplitude frequencies of FG beams exposed to varied end conditions, the Generalized Differential Quadrature Method (GDQM) accompiend by a precise and effective numerical method, is developed. Material properties change based on two models of power-law and exponential, in both thickness and axial directions of the beam. The technique's convergence behavior is proven by comparing the findings to other solutions for isotropic and FG beams. The results reveal that non-linear frequency ratios increase with increasing amplitude ratios and decrease with increasing elastic substrate stiffnesses. In addition, as porosities and material indexes increase in two directions, non-dimensional frequencies decrease sharply.

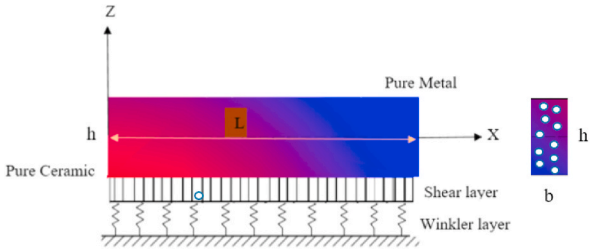

Fig. 1. Sketch of Bi-directional FG beam lying on substrate.

2. Theory and formulation

2.1. Kinematics and constitutive relations

An elastic Winkler and Shear substrate is applied to a two-directional functionally graded beam with length L and a rectangular cross-section b × h. As shown In Fig. 1, the length, width, and height of the beam are measured in Cartesian coordinates (x, y, z).

Using third-order shear deformation beam theories, displacement fields are selected according to the following assumptions. W_b and W_s are the bending and shear components of transverse displacement of a point on the mid-plane of the beam. In addition, the bending component of the axial displacement is similar to that supplied by the CBT. A bi-directional beam's top and bottom shear stresses should diminish as well. The shear component of the axial displacement generates the higher-order variation of shear strain across the depth of a beam. As a result of these assumptions, the displacement field may be represented as follows [1]:

$$\begin{aligned} U(x,z,t) &= u(x,t) - z\frac{\partial w_b(x,t)}{\partial x} - f(z)\frac{\partial w_s(x,t)}{\partial x} \\ W(x,z,t) &= w_b(x,t) + w_s(x,t) \end{aligned} \tag{1}$$

In this case, u represents the axial displacement of a point from the beam's midplane. In the midplane of a beam, the bending and shear components are W_b and W_s, respectively. The form function f illustrates how transverse shear stress and strain are distributed along FG beam's thickness direction f(z). Since the shape function f (z) fulfills the stress-free boundary conditions on the top and bottom surfaces of the beam, no shear correction factor is needed. This is supported by Reddy's third-order beam shear deformation theory [1]. F(z) can be expressed as follows Eq. (2):

$$f(z) = \frac{4z^3}{3h^2} \tag{2}$$

Considering the displacement field Eq. (1), The von Karman strain formula which is actually the non-zero components of the nonlinear Green's tensor, is derived in the form Eq. (3) [32,35,43,44]:

Eqs. (4) and (5) represent the non-zero stresses.

$$\varepsilon_x = \frac{\partial u}{\partial x} + \frac{1}{2}\left(\frac{\partial w}{\partial x}\right)^2 - z\frac{\partial^2 w}{\partial x^2} \tag{3}$$

$$\sigma_{xx} = E(x,z)\left(\begin{array}{l} -z\dfrac{\partial^2 w_b(x,t)}{\partial x^2} - f(z)\dfrac{\partial^2 w_s(x,t)}{\partial x^2} + \dfrac{\partial u(x,t)}{\partial x} + \dfrac{\partial w_b(x,t)}{\partial x}\dfrac{\partial w_s(x,t)}{\partial x} \\ +\dfrac{1}{2}\left(\dfrac{\partial w_b(x,t)}{\partial x}\right)^2 + \dfrac{1}{2}\left(\dfrac{\partial w_s(x,t)}{\partial x}\right)^2 \end{array}\right) \tag{4}$$

$$\sigma_{xz} = G(x,z)\left(\frac{\partial w_s(x,t)}{\partial x} - \frac{\partial f(z)}{\partial z}\frac{\partial w_s(x,t)}{\partial x}\right) = G(x,z)g(z)\frac{\partial w_s(x,t)}{\partial x} \tag{5}$$

2.2. Bi-directional FG material porous properties

According to the PFGM, metal and ceramic have variable volume fractions across thickness and axis as a result of the power-law distribution across the bi-directional beam (Fig. 1). Regarding the volume fractions of the constituents, specifically [26]:

$$\begin{aligned} &V_c + V_m = 1 \\ &V_c = \left(\frac{1}{2} + \frac{z}{h}\right)^{P_z}\left(\frac{x}{L}\right)^{P_x} \end{aligned} \tag{6}$$

where $-h/2 \prec z \prec h/2$ and p_x, p_z are the material power-law indexes along length and thickness direction respectively, which accept values that are larger than zero. A wholly ceramic beam is represented by p_x and p_z equal to zero, but a nearly entirely metallic beam is

shown by p_x and p_z close to infinity. The ceramic and metal volume fractions are indicated by the values V_c and V_m. Young's modulus E, Poisson's ratio ν, and e_0 stands for the porosity formation throughout manufacturing processes which is inevitable. The each property P (x,z) can be written as [27]:

$$P(x,z) = P_m\left(V_m - \frac{e_0}{2}\right) + P_c\left(V_c - \frac{e_0}{2}\right) \tag{7}$$

which designates the components made of metal and ceramic by the subscripts m and c. Young's modulus and mass density are stated as Eq. (8) [27] by substituting Eq. (6) into Eq. (7):

$$\begin{aligned} P(x,z) &= P_m + (P_c - P_m)\left(\frac{1}{2} + \frac{z}{h}\right)^{P_z}\left(\frac{x}{L}\right)^{P_x} - \frac{e_0}{2}(P_c + P_m) \\ E(x,z) &= E_m + (E_c - E_m)\left(\frac{1}{2} + \frac{z}{h}\right)^{P_z}\left(\frac{x}{L}\right)^{P_x} - \frac{e_0}{2}(E_c + E_m) \\ \rho(x,z) &= \rho_m + (\rho_c - \rho_m)\left(\frac{1}{2} + \frac{z}{h}\right)^{P_z}\left(\frac{x}{L}\right)^{P_x} - \frac{e_0}{2}(\rho_c + \rho_m) \end{aligned} \tag{8}$$

The fact that different kinds of functions are utilized to describe how the physical characteristics of FGM vary is also important to note. That is why, this paper utilizes an exponential function called the exponential function gradient model (EFGM) to explain the fluctuations in material traits that occur across the length and thickness of a beam. The EFGM is employed to capture the variability in porous material properties within the beam by using an exponential function Eq. (9) [45].

$$\begin{aligned} P(x,z) &= P_m(1 - \exp(e_0))e^{p_x\left(\frac{x}{L}+\frac{1}{2}\right)+p_z\left(\frac{z}{h}+\frac{1}{2}\right)} \\ E(x,z) &= E_m(1 - \exp(e_0))e^{p_x\left(\frac{x}{L}+\frac{1}{2}\right)+p_z\left(\frac{z}{h}+\frac{1}{2}\right)} \\ \rho(x,z) &= \rho_m(1 - \exp(e_0))e^{p_x\left(\frac{x}{L}+\frac{1}{2}\right)+p_z\left(\frac{z}{h}+\frac{1}{2}\right)} \end{aligned} \tag{9}$$

2.3. Fundamental formulations

2.3.1. Constitutive relations

From Hamilton's law, it is possible to infer the constitutive relations. This may be stated as follows Eq. (10) [1–4]

$$\int_{t1}^{t2}\left(\delta K - \delta U - \delta V_{ef}\right)dt = 0 \tag{10}$$

where t is the time, δK is the variation in kinetic energy, δU is the variation in strain energy, and δV_{ef} is the variation in potential energy of the elastic substrate.

The strain energy of mechanical stresses of the beam is presented as follows Eqs. (11) and (12) [1,3,4]

$$U = \frac{1}{2}\int_0^L\int_A (\sigma_{xx}\varepsilon_{xx} + \sigma_{xz}\varepsilon_{xz})\, dA dx \tag{11}$$

$$
\begin{aligned}
U = \int_0^L \Bigg[& A(x)\frac{\partial u(x,t)}{\partial x}\frac{\partial w_b(x,t)}{\partial x}\frac{\partial w_s(x,t)}{\partial x} + \frac{1}{2}A(x)\left(\frac{\partial w_b(x,t)}{\partial x}\right)^3\frac{\partial w_s(x,t)}{\partial x} + \frac{3}{4}A(x)\left(\frac{\partial w_b(x,t)}{\partial x}\right)^2\left(\frac{\partial w_s(x,t)}{\partial x}\right)^2 \\
& + \frac{1}{2}A(x)\frac{\partial w_b(x,t)}{\partial x}\left(\frac{\partial w_s(x,t)}{\partial x}\right)^3 + \frac{1}{2}A(x)\frac{\partial u(x,t)}{\partial x}\left(\frac{\partial w_b(x,t)}{\partial x}\right)^2 + \frac{1}{8}A(x)\left(\frac{\partial w_b(x,t)}{\partial x}\right)^4 + \frac{1}{8}A(x)\left(\frac{\partial w_s(x,t)}{\partial x}\right)^4 \\
& + \frac{1}{2}A(x)\frac{\partial u(x,t)}{\partial x}\left(\frac{\partial w_s(x,t)}{\partial x}\right)^2 + \frac{1}{2}A_s(x)\left(\frac{\partial w_s(x,t)}{\partial x}\right)^2 + \frac{1}{2}A(x)\left(\frac{\partial u(x,t)}{\partial x}\right)^2 + \frac{1}{2}D(x)\left(\frac{\partial^2 w_b(x,t)}{\partial x^2}\right)^2 - \\
& \frac{1}{2}B_s(x)\left(\frac{\partial w_b(x,t)}{\partial x}\right)^2\frac{\partial^2 w_s(x,t)}{\partial x^2} - B(x)\frac{\partial^2 w_b(x,t)}{\partial x^2}\frac{\partial w_b(x,t)}{\partial x}\frac{\partial w_s(x,t)}{\partial x} - B_s(x)\frac{\partial w_b(x,t)}{\partial x}\frac{\partial w_s(x,t)}{\partial x}\frac{\partial^2 w_s(x,t)}{\partial x^2} \\
& - \frac{1}{2}B(x)\frac{\partial^2 w_b(x,t)}{\partial x^2}\left(\frac{\partial w_s(x,t)}{\partial x}\right)^2 - B(x)\frac{\partial u(x,t)}{\partial x}\frac{\partial^2 w_b(x,t)}{\partial x^2} - \frac{1}{2}B(x)\frac{\partial^2 w_b(x,t)}{\partial x^2}\left(\frac{\partial w_b(x,t)}{\partial x}\right)^2 + \\
& D_s(x)\frac{\partial^2 w_b(x,t)}{\partial x^2}\frac{\partial^2 w_s(x,t)}{\partial x^2} - B_s(x)\frac{\partial u(x,t)}{\partial x}\frac{\partial^2 w_s(x,t)}{\partial x^2} - \frac{1}{2}B_s(x)\left(\frac{\partial w_s(x,t)}{\partial x}\right)^2\frac{\partial^2 w_s(x,t)}{\partial x^2} \\
& + \frac{1}{2}H_s(x)\left(\frac{\partial^2 w_s(x,t)}{\partial x^2}\right)^2\Bigg] dx
\end{aligned}
\tag{12}
$$

According to Ref. [1], the Kinetic energy and Potential one caused by the elastic substrate are Eqs. (13)–(16):

$$
K = \frac{1}{2}\int_0^L \int_A \rho(z)\left(\dot{U}^2 + \dot{W}^2\right) dA dx \tag{13}
$$

$$
\begin{aligned}
K = \int_0^L \Bigg[& J_2(x)\frac{\partial^2 w_b(x,t)}{\partial x \partial t}\frac{\partial^2 w_s(x,t)}{\partial x \partial t} - \mathscr{I}_1(x)\frac{\partial u(x,t)}{\partial t}\frac{\partial^2 w_b(x,t)}{\partial x \partial t} + \frac{1}{2}\mathscr{I}_2(x)\left(\frac{\partial^2 w_b(x,t)}{\partial x \partial t}\right)^2 \\
& - J_1(x)\frac{\partial u(x,t)}{\partial t}\frac{\partial^2 w_s(x,t)}{\partial x \partial t} + \frac{1}{2}K_2(x)\left(\frac{\partial^2 w_s(x,t)}{\partial x \partial t}\right)^2 + \mathscr{I}_0(x)\frac{\partial w_b(x,t)}{\partial t}\frac{\partial w_s(x,t)}{\partial t} + \\
& \frac{1}{2}\mathscr{I}_0(x)\left(\frac{\partial w_b(x,t)}{\partial t}\right)^2 + \frac{1}{2}\mathscr{I}_0(x)\left(\frac{\partial w_s(x,t)}{\partial t}\right)^2 + \frac{1}{2}\mathscr{I}_0(x)\left(\frac{\partial u(x,t)}{\partial t}\right)^2\Bigg] dx
\end{aligned}
\tag{14}
$$

$$
V_{ef} = \int_0^l \frac{1}{2}k_w(w_b + w_s)^2 + k_g\left(\frac{\partial w_b}{\partial x} + \frac{\partial w_s}{\partial x}\right)^2 + \frac{1}{4}k_N(w_b + w_s)^4 dx \tag{15}
$$

$$
\begin{aligned}
V_{ef} = \int_0^L \Bigg[& K_g\frac{\partial w_b(x,t)}{\partial x}\frac{\partial w_s(x,t)}{\partial x} + \frac{1}{2}K_g\left(\frac{\partial w_b(x,t)}{\partial x}\right)^2 + K_N w_b(x,t)^3 w_s(x,t) + \frac{3}{2}K_N w_b(x,t)^2 w_s(x,t)^2 + \\
& K_N w_b(x,t) w_s(x,t)^3 + \frac{1}{4}K_N w_b(x,t)^4 + K_w w_b(x,t) w_s(x,t) + \frac{1}{2}K_w w_b(x,t)^2 + \frac{1}{2}K_g\left(\frac{\partial w_s(x,t)}{\partial x}\right)^2 \\
& + \frac{1}{4}K_N w_s(x,t)^4 + \frac{1}{2}K_w w_s(x,t)^2\Bigg] dx
\end{aligned}
\tag{16}
$$

where the Winkler and shearing-layer elastic coefficients of the substrate, K_w and K_g, respectively, rely on the bed traits, such as the soil length, elastic modulus, and Poisson's ratio of the soil. The elastic foundation's nonlinear coefficient is K_N. The constitutive relations of the bi-directional beam are given below by inserting Eqs. (11)–(16) into Eq. (10) and integrating parts concerning spatial and time variables.

δu:

$$
\frac{\partial N_{xx}(x,t)}{\partial x} = \mathscr{I}_0(x)\frac{\partial^2 u(x,t)}{\partial t^2} - \mathscr{I}_1(x)\frac{\partial^3 w_b(x,t)}{\partial x \partial t^2} - J_1(x)\frac{\partial^3 w_s(x,t)}{\partial x \partial t^2} \tag{17}
$$

δw_b:

$$\begin{aligned}&\frac{\partial^2 M_b(x,t)}{\partial x^2}+N_{xx}(x,t)\frac{\partial^2 w_b(x,t)}{\partial x^2}+N_{xx}(x,t)\frac{\partial^2 w_s(x,t)}{\partial x^2}+\frac{\partial N_{xx}(x,t)}{\partial x}\frac{\partial w_s(x,t)}{\partial x}+\frac{\partial w_b(x,t)}{\partial x}\frac{\partial N_{xx}(x,t)}{\partial x}\\&\quad -K_w w_b(x,t)-K_w w_s(x,t)+K_g\frac{\partial^2 w_b(x,t)}{\partial x^2}+K_g\frac{\partial^2 w_s(x,t)}{\partial x^2}-K_N w_s(x,t)^3-K_N w_b(x,t)^3\\&-3K_N w_b(x,t)^2 w_s(x,t)-3K_N w_b(x,t)w_s(x,t)^2=\mathscr{I}_1(x)\frac{\partial^3 u(x,t)}{\partial x\partial t^2}+\frac{\partial \mathscr{I}_1(x)}{\partial x}\frac{\partial^2 u(x,t)}{\partial t^2}+\mathscr{I}_0(x)\frac{\partial^2 w_b(x,t)}{\partial t^2}\\&-\mathscr{I}_2(x)\frac{\partial^4 w_b(x,t)}{\partial x^2\partial t^2}-\frac{\partial \mathscr{I}_2(x)}{\partial x}\frac{\partial^3 w_b(x,t)}{\partial x\partial t^2}+\mathscr{I}_0(x)\frac{\partial^2 w_s(x,t)}{\partial t^2}-J_2(x)\frac{\partial^4 w_s(x,t)}{\partial x^2\partial t^2}-\frac{\partial J_2(x)}{\partial x}\frac{\partial^3 w_s(x,t)}{\partial x\partial t^2}\end{aligned}\tag{18}$$

δw_s:

$$\begin{aligned}&\frac{\partial Q_{xz}(x,t)}{\partial x}+\frac{\partial^2 M_S(x,t)}{\partial x^2}+N_{xx}(x,t)\frac{\partial^2 w_b(x,t)}{\partial x^2}+N_{xx}(x,t)\frac{\partial^2 w_s(x,t)}{\partial x^2}+\frac{\partial w_b(x,t)}{\partial x}\frac{\partial N_{xx}(x,t)}{\partial x}\\&\quad+\frac{\partial N_{xx}(x,t)}{\partial x}\frac{\partial w_s(x,t)}{\partial x}-K_w w_s(x,t)-K_w w_b(x,t)+K_g\frac{\partial^2 w_b(x,t)}{\partial x^2}+K_g\frac{\partial^2 w_s(x,t)}{\partial x^2}\\&\quad-K_N w_s(x,t)^3-K_N w_b(x,t)^3-3K_N w_b(x,t)^2 w_s(x,t)-3K_N w_b(x,t)w_s(x,t)^2\\&\quad=J_1(x)\frac{\partial^3 u(x,t)}{\partial x\partial t^2}+\frac{\partial J_1(x)}{\partial x}\frac{\partial^2 u(x,t)}{\partial t^2}+\mathscr{I}_0(x)\frac{\partial^2 w_b(x,t)}{\partial t^2}-\frac{\partial J_2(x)}{\partial x}\frac{\partial^3 w_b(x,t)}{\partial x\partial t^2}\\&\quad-J_2(x)\frac{\partial^4 w_b(x,t)}{\partial x^2\partial t^2}+\mathscr{I}_0(x)\frac{\partial^2 w_s(x,t)}{\partial t^2}-K_2(x)\frac{\partial^4 w_s(x,t)}{\partial x^2\partial t^2}-\frac{\partial K_2(x)}{\partial x}\frac{\partial^3 w_s(x,t)}{\partial x\partial t^2}\end{aligned}\tag{19}$$

The parameters N_{xx}; M_b; M_s Eqs. (20)–(23) and other stress resultants are extracted as Eqs. (24) and (25):

$$N_{xx}=A(x)\frac{\partial w_b(x,t)}{\partial x}\frac{\partial w_s(x,t)}{\partial x}+\frac{1}{2}A(x)\left(\frac{\partial w_b(x,t)}{\partial x}\right)^2+\frac{1}{2}A(x)\left(\frac{\partial w_s(x,t)}{\partial x}\right)^2+A(x)\frac{\partial u(x,t)}{\partial x}-B(x)\frac{\partial^2 w_b(x,t)}{\partial x^2}-B_s(x)\frac{\partial^2 w_s(x,t)}{\partial x^2}\tag{20}$$

$$M_b=B(x)\frac{\partial w_b(x,t)}{\partial x}\frac{\partial w_s(x,t)}{\partial x}+\frac{1}{2}B(x)\left(\frac{\partial w_b(x,t)}{\partial x}\right)^2-D(x)\frac{\partial^2 w_b(x,t)}{\partial x^2}+\frac{1}{2}B(x)\left(\frac{\partial w_s(x,t)}{\partial x}\right)^2+B(x)\frac{\partial u(x,t)}{\partial x}-D_s(x)\frac{\partial^2 w_s(x,t)}{\partial x^2}\tag{21}$$

$$M_S=\frac{1}{2}B_s(x)\left(\frac{\partial w_b(x,t)}{\partial x}\right)^2+B_s(x)\frac{\partial w_b(x,t)}{\partial x}\frac{\partial w_s(x,t)}{\partial x}-D_s(x)\frac{\partial^2 w_b(x,t)}{\partial x^2}+B_s(x)\frac{\partial u(x,t)}{\partial x}+\frac{1}{2}B_s(x)\left(\frac{\partial w_s(x,t)}{\partial x}\right)^2-H_s(x)\frac{\partial^2 w_s(x,t)}{\partial x^2}\tag{22}$$

$$Q_{xz}=g(z)^2G(x,z)\frac{\partial w_s(x,t)}{\partial x}\tag{23}$$

where

$$\begin{aligned}\mathscr{I}_0(x)&=\int_{-b/2}^{b/2}\int_{-h/2}^{h/2}\rho(x,z)dA\\\mathscr{I}_1(x)&=\int_{-b/2}^{b/2}\int_{-h/2}^{h/2}z\rho(x,z)dA\\\mathscr{I}_2(x)&=\int_{-b/2}^{b/2}\int_{-h/2}^{h/2}z^2\rho(x,z)dA\\J_1(x)&=\int_{-b/2}^{b/2}\int_{-h/2}^{h/2}f(z)\rho(x,z)dA\\J_2(x)&=\int_{-b/2}^{b/2}\int_{-h/2}^{h/2}zf(z)\rho(x,z)dA\\K_2(x)&=\int_{-b/2}^{b/2}\int_{-h/2}^{h/2}f(z)^2\rho(x,z)dA\end{aligned}\tag{24}$$

$$
\begin{aligned}
A(x) &= \int_{-b/2}^{b/2}\int_{-h/2}^{h/2} E(x,z)dA \\
B(x) &= \int_{-b/2}^{b/2}\int_{-h/2}^{h/2} zE(x,z)dA \\
D(x) &= \int_{-b/2}^{b/2}\int_{-h/2}^{h/2} z^2E(x,z)dA \\
A_s(x) &= \int_{-b/2}^{b/2}\int_{-h/2}^{h/2} g(z)^2G(x,z)dA \\
B_s(x) &= \int_{-b/2}^{b/2}\int_{-h/2}^{h/2} f(z)E(x,z)dA \\
D_s(x) &= \int_{-b/2}^{b/2}\int_{-h/2}^{h/2} zf(z)E(x,z)dA \\
H_s(x) &= \int_{-b/2}^{b/2}\int_{-h/2}^{h/2} f(z)^2E(x,z)dA
\end{aligned}
\tag{25}
$$

The constitutive relations can be constructed regarding the displacements as follows Eqs. (26)–(28) by inserting the stress resultants in Eqs. (20)–(23) into Eqs. (17)–(19).

δu:

$$
\begin{aligned}
&A(x)\frac{\partial^2 u(x,t)}{\partial x^2}+\frac{\partial A(x)}{\partial x}\frac{\partial u(x,t)}{\partial x}+\frac{\partial^2 w_b(x,t)}{\partial x^2}\left(A(x)\frac{\partial w_b(x,t)}{\partial x}+A(x)\frac{\partial w_s(x,t)}{\partial x}-\frac{\partial B(x)}{\partial x}\right)+\frac{1}{2}\frac{\partial A(x)}{\partial x}\left(\frac{\partial w_b(x,t)}{\partial x}\right)^2 \\
&\quad -B(x)\frac{\partial^3 w_b(x,t)}{\partial x^3}+\frac{\partial^2 w_s(x,t)}{\partial x^2}\left(A(x)\frac{\partial w_b(x,t)}{\partial x}+A(x)\frac{\partial w_s(x,t)}{\partial x}-\frac{\partial B_s(x)}{\partial x}\right)+\frac{1}{2}\frac{\partial A(x)}{\partial x}\left(\frac{\partial w_s(x,t)}{\partial x}\right)^2 \\
&\quad -B_s(x)\frac{\partial^3 w_s(x,t)}{\partial x^3}+\frac{\partial A(x)}{\partial x}\frac{\partial w_b(x,t)}{\partial x}\frac{\partial w_s(x,t)}{\partial x}=\mathcal{J}_0(x)\frac{\partial^2 u(x,t)}{\partial t^2}-\mathcal{J}_1(x)\frac{\partial^3 w_b(x,t)}{\partial x\partial t^2}-J_1(x)\frac{\partial^3 w_s(x,t)}{\partial x\partial t^2}
\end{aligned}
\tag{26}
$$

δw_b:

$$
\begin{aligned}
&B(x)\frac{\partial^3 u(x,t)}{\partial x^3}+\frac{\partial^2 u(x,t)}{\partial x^2}\left(2\frac{\partial B(x)}{\partial x}+A(x)\frac{\partial w_b(x,t)}{\partial x}+A(x)\frac{\partial w_s(x,t)}{\partial x}\right)+\\
&\frac{\partial u(x,t)}{\partial x}\left(\frac{\partial^2 B(x)}{\partial x^2}+\frac{\partial A(x)}{\partial x}\frac{\partial w_b(x,t)}{\partial x}+A(x)\frac{\partial^2 w_b(x,t)}{\partial x^2}+\frac{\partial A(x)}{\partial x}\frac{\partial w_s(x,t)}{\partial x}+A(x)\frac{\partial^2 w_s(x,t)}{\partial x^2}\right)\\
&+\frac{1}{2}\frac{\partial A(x)}{\partial x}\left(\frac{\partial w_b(x,t)}{\partial x}\right)^3+\frac{1}{2}\frac{\partial^2 B(x)}{\partial x^2}\left(\frac{\partial w_b(x,t)}{\partial x}\right)^2+\frac{3}{2}\frac{\partial A(x)}{\partial x}\frac{\partial w_s(x,t)}{\partial x}\left(\frac{\partial w_b(x,t)}{\partial x}\right)^2\\
&+\frac{3}{2}\frac{\partial A(x)}{\partial x}\left(\frac{\partial w_s(x,t)}{\partial x}\right)^2\frac{\partial w_b(x,t)}{\partial x}+\frac{\partial^2 B(x)}{\partial x^2}\frac{\partial w_s(x,t)}{\partial x}\frac{\partial w_b(x,t)}{\partial x}-2\frac{\partial D(x)}{\partial x}\frac{\partial^3 w_b(x,t)}{\partial x^3}-D(x)\frac{\partial^4 w_b(x,t)}{\partial x^4}\\
&+\frac{\partial^2 w_b(x,t)}{\partial x^2}\left(\frac{3}{2}A(x)\left(\frac{\partial w_b(x,t)}{\partial x}\right)^2+\frac{\partial B(x)}{\partial x}\frac{\partial w_b(x,t)}{\partial x}+3A(x)\frac{\partial w_s(x,t)}{\partial x}\frac{\partial w_b(x,t)}{\partial x}\right.\\
&\left.+\frac{3}{2}A(x)\left(\frac{\partial w_s(x,t)}{\partial x}\right)^2-\frac{\partial^2 D(x)}{\partial x^2}+\frac{\partial B(x)}{\partial x}\frac{\partial w_s(x,t)}{\partial x}+K_g+\frac{\partial^2 w_s(x,t)}{\partial x^2}(B(x)-B_s(x))\right)\\
&+\frac{1}{2}\frac{\partial A(x)}{\partial x}\left(\frac{\partial w_s(x,t)}{\partial x}\right)^3+\frac{1}{2}\frac{\partial^2 B(x)}{\partial x^2}\left(\frac{\partial w_s(x,t)}{\partial x}\right)^2+\frac{\partial^2 w_s(x,t)}{\partial x^2}\left(\frac{3}{2}A(x)\left(\frac{\partial w_b(x,t)}{\partial x}\right)^2\right.\\
&+2\frac{\partial B(x)}{\partial x}\frac{\partial w_b(x,t)}{\partial x}-\frac{\partial B_s(x)}{\partial x}\frac{\partial w_b(x,t)}{\partial x}+3A(x)\frac{\partial w_s(x,t)}{\partial x}\frac{\partial w_b(x,t)}{\partial x}\\
&\left.+\frac{3}{2}A(x)\left(\frac{\partial w_s(x,t)}{\partial x}\right)^2+2\frac{\partial B(x)}{\partial x}\frac{\partial w_s(x,t)}{\partial x}-\frac{\partial B_s(x)}{\partial x}\frac{\partial w_s(x,t)}{\partial x}-\frac{\partial^2 D_s(x)}{\partial x^2}+K_g\right)+\\
&\left(\frac{\partial^2 w_s(x,t)}{\partial x^2}\right)^2(B(x)-B_s(x))+\frac{\partial^3 w_s(x,t)}{\partial x^3}\left(B(x)\frac{\partial w_b(x,t)}{\partial x}-B_s(x)\frac{\partial w_b(x,t)}{\partial x}\right.\\
&\left.+B(x)\frac{\partial w_s(x,t)}{\partial x}-2\frac{\partial D_s(x)}{\partial x}-\frac{\partial w_s(x,t)}{\partial x}B_s(x)\right)-K_N w_b(x,t)^3-K_N w_s(x,t)^3-\\
&3K_N w_b(x,t)^2 w_s(x,t)-K_w w_s(x,t)+w_b(x,t)\left(-3K_N w_s(x,t)^2-K_w\right)-\frac{\partial^4 w_s(x,t)}{\partial x^4}D_s(x)\\
&=\mathscr{I}_1(x)\frac{\partial^3 u(x,t)}{\partial x\partial t^2}+\frac{\partial \mathscr{I}_1(x)}{\partial x}\frac{\partial^2 u(x,t)}{\partial t^2}+\mathscr{I}_0(x)\frac{\partial^2 w_b(x,t)}{\partial t^2}-\mathscr{I}_2(x)\frac{\partial^4 w_b(x,t)}{\partial x^2\partial t^2}\\
&-\frac{\partial \mathscr{I}_2(x)}{\partial x}\frac{\partial^3 w_b(x,t)}{\partial x\partial t^2}+\mathscr{I}_0(x)\frac{\partial^2 w_s(x,t)}{\partial t^2}-J_2(x)\frac{\partial^4 w_s(x,t)}{\partial x^2\partial t^2}-\frac{\partial J_2(x)}{\partial x}\frac{\partial^3 w_s(x,t)}{\partial x\partial t^2}
\end{aligned}
\tag{27}
$$

δw_s:

$$
\begin{aligned}
&B_s(x)\frac{\partial^3 u(x,t)}{\partial x^3}+A(x)\frac{\partial^2 u(x,t)}{\partial x^2}\frac{\partial w_s(x,t)}{\partial x}+A(x)\frac{\partial u(x,t)}{\partial x}\frac{\partial^2 w_s(x,t)}{\partial x^2}+2\frac{\partial B_s(x)}{\partial x}\frac{\partial^2 u(x,t)}{\partial x^2}+\frac{\partial^2 B_s(x)}{\partial x^2}\frac{\partial u(x,t)}{\partial x}\\
&+A(x)\frac{\partial u(x,t)}{\partial x}\frac{\partial^2 w_b(x,t)}{\partial x^2}+\frac{\partial A(x)}{\partial x}\frac{\partial u(x,t)}{\partial x}\frac{\partial w_s(x,t)}{\partial x}+A(x)\frac{\partial^2 u(x,t)}{\partial x^2}\frac{\partial w_b(x,t)}{\partial x}+\frac{\partial A(x)}{\partial x}\frac{\partial u(x,t)}{\partial x}\frac{\partial w_b(x,t)}{\partial x}+\\
&\frac{1}{2}\frac{\partial A(x)}{\partial x}\left(\frac{\partial w_b(x,t)}{\partial x}\right)^3+\frac{1}{2}\frac{\partial^2 B_s(x)}{\partial x^2}\left(\frac{\partial w_b(x,t)}{\partial x}\right)^2+\frac{3}{2}A(x)\frac{\partial^2 w_b(x,t)}{\partial x^2}\left(\frac{\partial w_b(x,t)}{\partial x}\right)^2\\
&+\frac{3}{2}\frac{\partial A(x)}{\partial x}\frac{\partial w_s(x,t)}{\partial x}\left(\frac{\partial w_b(x,t)}{\partial x}\right)^2+\frac{3}{2}A(x)\frac{\partial^2 w_s(x,t)}{\partial x^2}\left(\frac{\partial w_b(x,t)}{\partial x}\right)^2+\frac{3}{2}\frac{\partial A(x)}{\partial x}\left(\frac{\partial w_s(x,t)}{\partial x}\right)^2\frac{\partial w_b(x,t)}{\partial x}-\\
&\frac{\partial B(x)}{\partial x}\frac{\partial^2 w_b(x,t)}{\partial x^2}\frac{\partial w_b(x,t)}{\partial x}+2\frac{\partial B_s(x)}{\partial x}\frac{\partial^2 w_b(x,t)}{\partial x^2}\frac{\partial w_b(x,t)}{\partial x}-B(x)\frac{\partial^3 w_b(x,t)}{\partial x^3}\frac{\partial w_b(x,t)}{\partial x}+\\
&3A(x)\frac{\partial^2 w_b(x,t)}{\partial x^2}\frac{\partial w_s(x,t)}{\partial x}\frac{\partial w_b(x,t)}{\partial x}-\frac{\partial B_s(x)}{\partial x}\frac{\partial^2 w_s(x,t)}{\partial x^2}\frac{\partial w_b(x,t)}{\partial x}+3A(x)\frac{\partial w_s(x,t)}{\partial x}\frac{\partial^2 w_s(x,t)}{\partial x^2}\frac{\partial w_b(x,t)}{\partial x}\\
&-D_s(x)\frac{\partial^4 w_b(x,t)}{\partial x^4}+\frac{3}{2}A(x)\frac{\partial^2 w_b(x,t)}{\partial x^2}\left(\frac{\partial w_s(x,t)}{\partial x}\right)^2-\frac{\partial B(x)}{\partial x}\frac{\partial^2 w_b(x,t)}{\partial x^2}\frac{\partial w_s(x,t)}{\partial x}-2\frac{\partial D_s(x)}{\partial x}\frac{\partial^3 w_b(x,t)}{\partial x^3}\\
&-\frac{\partial^2 D_s(x)}{\partial x^2}\frac{\partial^2 w_b(x,t)}{\partial x^2}-B_s(x)\frac{\partial^2 w_b(x,t)}{\partial x^2}\frac{\partial^2 w_s(x,t)}{\partial x^2}-B(x)\frac{\partial^2 w_b(x,t)}{\partial x^2}\frac{\partial^2 w_s(x,t)}{\partial x^2}-B(x)\frac{\partial^3 w_b(x,t)}{\partial x^3}\frac{\partial w_s(x,t)}{\partial x}\\
&-B(x)\left(\frac{\partial^2 w_b(x,t)}{\partial x^2}\right)^2+\frac{1}{2}\frac{\partial^2 B_s(x)}{\partial x^2}\left(\frac{\partial w_s(x,t)}{\partial x}\right)^2+\frac{1}{2}\frac{\partial A(x)}{\partial x}\left(\frac{\partial w_s(x,t)}{\partial x}\right)^3+\frac{\partial A_s(x)}{\partial x}\frac{\partial w_s(x,t)}{\partial x}+\\
&\frac{3}{2}A(x)\left(\frac{\partial w_s(x,t)}{\partial x}\right)^2\frac{\partial^2 w_s(x,t)}{\partial x^2}+\frac{\partial B_s(x)}{\partial x}\frac{\partial w_s(x,t)}{\partial x}\frac{\partial^2 w_s(x,t)}{\partial x^2}-2\frac{\partial H_s(x)}{\partial x}\frac{\partial^3 w_s(x,t)}{\partial x^3}-\frac{\partial^2 H_s(x)}{\partial x^2}\frac{\partial^2 w_s(x,t)}{\partial x^2}+\\
&\frac{\partial K_2(x)}{\partial x}\frac{\partial^3 w_s(x,t)}{\partial x\partial t^2}+A_s(x)\frac{\partial^2 w_s(x,t)}{\partial x^2}-B_s(x)\left(\frac{\partial^2 w_s(x,t)}{\partial x^2}\right)^2+B_s(x)\left(\left(\frac{\partial^2 w_b(x,t)}{\partial x^2}\right)^2+\frac{\partial w_b(x,t)}{\partial x}\frac{\partial^3 w_b(x,t)}{\partial x^3}\right)\\
&-B_s(x)\frac{\partial w_s(x,t)}{\partial x}\frac{\partial^3 w_s(x,t)}{\partial x^3}+\frac{\partial w_s(x,t)}{\partial x}\left(\frac{\partial^2 B_s(x)}{\partial x^2}\frac{\partial w_b(x,t)}{\partial x}+2\frac{\partial B_s(x)}{\partial x}\frac{\partial^2 w_b(x,t)}{\partial x^2}+B_s(x)\frac{\partial^3 w_b(x,t)}{\partial x^3}\right)\\
&+2\frac{\partial^2 w_s(x,t)}{\partial x^2}\left(\frac{\partial B_s(x)}{\partial x}\frac{\partial w_b(x,t)}{\partial x}+B_s(x)\frac{\partial^2 w_b(x,t)}{\partial x^2}\right)+B_s(x)\left(\left(\frac{\partial^2 w_s(x,t)}{\partial x^2}\right)^2+\frac{\partial w_s(x,t)}{\partial x}\frac{\partial^3 w_s(x,t)}{\partial x^3}\right)\\
&-K_w w_b(x,t)-3K_N w_b(x,t)^2 w_s(x,t)-K_w w_s(x,t)-K_N w_b(x,t)^3-K_N w_s(x,t)^3-3K_N w_b(x,t)w_s(x,t)^2\\
&+K_g\frac{\partial^2 w_s(x,t)}{\partial x^2}+K_g\frac{\partial^2 w_b(x,t)}{\partial x^2}=J_1(x)\frac{\partial^3 u(x,t)}{\partial x\partial t^2}+\frac{\partial J_1(x)}{\partial x}\frac{\partial^2 u(x,t)}{\partial t^2}+\mathscr{I}_0(x)\frac{\partial^2 w_b(x,t)}{\partial t^2}-\frac{\partial J_2(x)}{\partial x}\frac{\partial^3 w_b(x,t)}{\partial x\partial t^2}\\
&-J_2(x)\frac{\partial^4 w_b(x,t)}{\partial x^2\partial t^2}+\mathscr{I}_0(x)\frac{\partial^2 w_s(x,t)}{\partial t^2}-K_2(x)\frac{\partial^4 w_s(x,t)}{\partial x^2\partial t^2}+H_s(x)\frac{\partial^4 w_s(x,t)}{\partial x^4}
\end{aligned}
\tag{28}
$$

2.3.2. End conditions

The following end conditions for the bi-directional beam's boundary conditions may be condensed to Eqs. (29)–(33):

$$
\begin{aligned}
u=0\quad \text{or}\quad &-A(x)\frac{\partial w_b(x,t)}{\partial x}\frac{\partial w_s(x,t)}{\partial x}-\frac{1}{2}A(x)\left(\frac{\partial w_b(x,t)}{\partial x}\right)^2-\frac{1}{2}A(x)\left(\frac{\partial w_s(x,t)}{\partial x}\right)^2-A(x)\frac{\partial u(x,t)}{\partial x}\\
&+B(x)\frac{\partial^2 w_b(x,t)}{\partial x^2}+B_s(x)\frac{\partial^2 w_s(x,t)}{\partial x^2}=0
\end{aligned}
\tag{29}
$$

$$
\begin{aligned}
\frac{\partial w_s}{\partial x}=0\quad \text{or}\quad &\frac{1}{2}B_s(x)\left(\frac{\partial w_b(x,t)}{\partial x}\right)^2+B_s(x)\frac{\partial w_b(x,t)}{\partial x}\frac{\partial w_s(x,t)}{\partial x}-D_s(x)\frac{\partial^2 w_b(x,t)}{\partial x^2}+B_s(x)\frac{\partial u(x,t)}{\partial x}\\
&+\frac{1}{2}B_s(x)\left(\frac{\partial w_s(x,t)}{\partial x}\right)^2-H_s(x)\frac{\partial^2 w_s(x,t)}{\partial x^2}=0
\end{aligned}
\tag{30}
$$

$$
\begin{aligned}
\frac{\partial w_b}{\partial x}=0\quad \text{or}\quad &B(x)\frac{\partial w_b(x,t)}{\partial x}\frac{\partial w_s(x,t)}{\partial x}+\frac{1}{2}B(x)\left(\frac{\partial w_b(x,t)}{\partial x}\right)^2-D(x)\frac{\partial^2 w_b(x,t)}{\partial x^2}+\frac{1}{2}B(x)\left(\frac{\partial w_s(x,t)}{\partial x}\right)^2\\
&+B(x)\frac{\partial u(x,t)}{\partial x}-D_s(x)\frac{\partial^2 w_s(x,t)}{\partial x^2}=0
\end{aligned}
\tag{31}
$$

$$
\begin{aligned}
&w_s = 0 \quad \text{or} \quad J_2(x)\frac{\partial^3 w_b(x,t)}{\partial x \partial t^2} + K_2(x)\frac{\partial^3 w_s(x,t)}{\partial x \partial t^2} + \frac{3}{2}A(x)\left(\frac{\partial w_b(x,t)}{\partial x}\right)^2 \frac{\partial w_s(x,t)}{\partial x} \\
&+\frac{3}{2}A(x)\frac{\partial w_b(x,t)}{\partial x}\left(\frac{\partial w_s(x,t)}{\partial x}\right)^2 + A(x)\frac{\partial u(x,t)}{\partial x}\frac{\partial w_b(x,t)}{\partial x} + \frac{1}{2}A(x)\left(\frac{\partial w_b(x,t)}{\partial x}\right)^3 + \\
&A(x)\frac{\partial u(x,t)}{\partial x}\frac{\partial w_s(x,t)}{\partial x} + \frac{1}{2}A(x)\left(\frac{\partial w_s(x,t)}{\partial x}\right)^3 + A_s(x)\frac{\partial w_s(x,t)}{\partial x} + B_s(x)\frac{\partial^2 w_b(x,t)}{\partial x^2}\frac{\partial w_b(x,t)}{\partial x} \\
&-B(x)\frac{\partial^2 w_b(x,t)}{\partial x^2}\frac{\partial w_s(x,t)}{\partial x} + B_s(x)\frac{\partial^2 w_b(x,t)}{\partial x^2}\frac{\partial w_s(x,t)}{\partial x} + \frac{1}{2}\frac{\partial B_s(x)}{\partial x}\left(\frac{\partial w_b(x,t)}{\partial x}\right)^2 + \\
&\frac{\partial B_s(x)}{\partial x}\frac{\partial w_b(x,t)}{\partial x}\frac{\partial w_s(x,t)}{\partial x} - B(x)\frac{\partial^2 w_b(x,t)}{\partial x^2}\frac{\partial w_b(x,t)}{\partial x} + K_g\frac{\partial w_b(x,t)}{\partial x} - D_s(x)\frac{\partial^3 w_b(x,t)}{\partial x^3} - \\
&\frac{\partial D_s(x)}{\partial x}\frac{\partial^2 w_b(x,t)}{\partial x^2} + B_s(x)\frac{\partial^2 u(x,t)}{\partial x^2} + \frac{\partial B_s(x)}{\partial x}\frac{\partial u(x,t)}{\partial x} + \frac{1}{2}\frac{\partial B_s(x)}{\partial x}\left(\frac{\partial w_s(x,t)}{\partial x}\right)^2 \\
&+K_g\frac{\partial w_s(x,t)}{\partial x} - J_1(x)\frac{\partial^2 u(x,t)}{\partial t^2} - H_s(x)\frac{\partial^3 w_s(x,t)}{\partial x^3} - \frac{\partial H_s(x)}{\partial x}\frac{\partial^2 w_s(x,t)}{\partial x^2} = 0
\end{aligned}
\tag{32}
$$

$$
\begin{aligned}
&w_b = 0 \quad \text{or} \quad \mathscr{J}_2(x)\frac{\partial^3 w_b(x,t)}{\partial x \partial t^2} + J_2(x)\frac{\partial^3 w_s(x,t)}{\partial x \partial t^2} + \frac{3}{2}A(x)\left(\frac{\partial w_b(x,t)}{\partial x}\right)^2 \frac{\partial w_s(x,t)}{\partial x} + \\
&\frac{3}{2}A(x)\frac{\partial w_b(x,t)}{\partial x}\left(\frac{\partial w_s(x,t)}{\partial x}\right)^2 + A(x)\frac{\partial u(x,t)}{\partial x}\frac{\partial w_b(x,t)}{\partial x} + \frac{1}{2}A(x)\left(\frac{\partial w_b(x,t)}{\partial x}\right)^3 + \\
&A(x)\frac{\partial u(x,t)}{\partial x}\frac{\partial w_s(x,t)}{\partial x} + \frac{1}{2}A(x)\left(\frac{\partial w_s(x,t)}{\partial x}\right)^3 + B(x)\frac{\partial w_b(x,t)}{\partial x}\frac{\partial^2 w_s(x,t)}{\partial x^2} - \\
&B_s(x)\frac{\partial w_b(x,t)}{\partial x}\frac{\partial^2 w_s(x,t)}{\partial x^2} + \frac{\partial B(x)}{\partial x}\frac{\partial w_b(x,t)}{\partial x}\frac{\partial w_s(x,t)}{\partial x} + \frac{1}{2}\frac{\partial B(x)}{\partial x}\left(\frac{\partial w_b(x,t)}{\partial x}\right)^2 + \\
&K_g\frac{\partial w_b(x,t)}{\partial x} - D(x)\frac{\partial^3 w_b(x,t)}{\partial x^3} - \frac{\partial D(x)}{\partial x}\frac{\partial^2 w_b(x,t)}{\partial x^2} + B(x)\frac{\partial w_s(x,t)}{\partial x}\frac{\partial^2 w_s(x,t)}{\partial x^2} - \\
&B_s(x)\frac{\partial w_s(x,t)}{\partial x}\frac{\partial^2 w_s(x,t)}{\partial x^2} + \frac{1}{2}\frac{\partial B(x)}{\partial x}\left(\frac{\partial w_s(x,t)}{\partial x}\right)^2 + B(x)\frac{\partial^2 u(x,t)}{\partial x^2} + \\
&\frac{\partial B(x)}{\partial x}\frac{\partial u(x,t)}{\partial x} + K_g\frac{\partial w_s(x,t)}{\partial x} - D_s(x)\frac{\partial^3 w_s(x,t)}{\partial x^3} - \frac{\partial D_s(x)}{\partial x}\frac{\partial^2 w_s(x,t)}{\partial x^2} - \mathscr{J}_1(x)\frac{\partial^2 u(x,t)}{\partial t^2} = 0
\end{aligned}
\tag{33}
$$

The following solutions may be taken into account for the displacement components in free vibration analysis.

2.4. Numerical solution method

The constitutive equations and associated end conditions are converted into algebraic equations using the Generalized Differential Quadrature (GDQ), wheras the discretization procedures follow Gauss-Lobatto-Chebyshev sampling points Eq. (34) [1,34].

$$
x_i = \frac{1}{2}\left\{1 - \cos\left(\frac{i-1}{N-1}\right)\pi\right\} \quad i = 1, 2, \ldots, N-1 \tag{34}
$$

Take x_i the discrete point, the nth-order partial differential of f(x) concerning x is Eq. (35):

$$
f_x^{(n)}(x_i) = \sum_{i=1}^{N} C_{ij}^{(n)} f(x_i) \tag{35}
$$

where N is designated as the number of grids in the x direction of the GDQ domain. $C_{ij}^{(n)}$ Eqs. (36) and (37) are weighting coefficients related to the discrete point x_i. The nth-order partial differential of f(x) concerning x. Here is the first [1,33,35]:

$$
C_{ij}^{1} = \frac{M(x_i)}{(x_i - x_j)M(x_j)} \tag{36}
$$

where

$$
M(x_i) = \prod_{j=1 \; j\neq i}^{N} (x_i - x_j) \tag{37}
$$

The following recurrence relation can be used to determine the weighting coefficients of higher-order derivatives. Eqs. (38) and (39)

$$C_{ij}^{(n)} = n\left(C_{ij}^{(n-1)}C_{ij}^{1} - \frac{C_{ij}^{(n-1)}}{(x_i - x_j)}\right) \quad i,j = 1,2,...N \tag{38}$$

$$C_{ij}^{(n)} = -\sum_{\substack{j=1 \\ j\neq i}}^{N} C_{ij}^{n} \quad n = 1,2,...N-1 \tag{39}$$

The partial derivatives of a function can be expressed as Eq. (40) [33,35,46,47] using this methodology:

$$\begin{aligned}
&\frac{\partial f(x,t)}{\partial x}|_{x=x_i} = \sum_{j=1}^{N} A_{ij} f(x_j,t) \quad i = 1,2,...,N \\
&\frac{\partial f^2(x,t)}{\partial x^2}|_{x=x_i} = \sum_{j=1}^{N} B_{ij} f(x_j,t) \\
&\frac{\partial f^3(x,t)}{\partial x^3}|_{x=x_i} = \sum_{j=1}^{N} C_{ij} f(x_j,t) \\
&\frac{\partial f^4(x,t)}{\partial x^4}|_{x=x_i} = \sum_{j=1}^{N} D_{ij} f(x_j,t)
\end{aligned} \tag{40}$$

where A_{ij}; B_{ij}; C_{ij}; D_{ij} are the first, second, third, and fourth-order weighting coefficients of the DQM, respectively Eq. (41) [33,46,47].

$$\begin{aligned}
[B_{ij}] &= [A_{ij}][A_{ij}] = [A_{ij}]^2, \\
[C_{ij}] &= [A_{ij}][B_{ij}] = [A_{ij}]^3, \\
[D_{ij}] &= [B_{ij}][B_{ij}] = [A_{ij}]^4
\end{aligned} \tag{41}$$

The GDQ approach may be used to obtain the nonlinear constitutive differential equations of motion's discrete form Eqs. (42)–(46)

δu:

$$\begin{aligned}
&\sum_{j=1}^{N}\Bigg\{(A_iB_{ij} + \widetilde{A}_iA_{ij})u_j + \left[\frac{1}{2}A_iA_{ij}\left(\sum_{k=1}^{N} B_{ik}w_{bk}\right) + \frac{1}{2}A_iA_{ij}\left(\sum_{k=1}^{N} B_{ik}w_{sk}\right) + \frac{1}{2}(A_iB_{ij} + \widetilde{A}_iA_{ij})\sum_{k=1}^{N} A_{ik}w_{bk}\right. \\
&+\frac{1}{2}(A_iB_{ij} + \widetilde{A}_iA_{ij})\left(\sum_{k=1}^{N} A_{ik}w_{sk}\right) - B_iC_{ij} - \widetilde{B}_iB_{ij}\Bigg]w_{bj} + \left[\frac{1}{2}A_iA_{ij}\left(\sum_{k=1}^{N} B_{ik}w_{bk}\right) + \frac{1}{2}A_iA_{ij}\left(\sum_{k=1}^{N} B_{ik}w_{sk}\right)\right. \\
&\left.+\frac{1}{2}(A_iB_{ij} + \widetilde{A}_iA_{ij})\sum_{k=1}^{N} A_{ik}w_{bk} + \frac{1}{2}(A_iB_{ij} + \widetilde{A}_iA_{ij})\sum_{k=1}^{N} A_{ik}w_{sk} - \widetilde{B}_{si}B_{ij} - B_{si}C_{ij}\Bigg]w_{sj}\Bigg\} \\
&= \mathscr{I}_{0i}\frac{d^2u_i}{dt^2} - \mathscr{I}_{1i}\sum_{j=1}^{N} A_{ij}\frac{d^2w_{bj}}{dt^2} - J_{1i}\sum_{j=1}^{N} A_{ij}\frac{d^2w_{sj}}{dt^2}
\end{aligned} \tag{42}$$

δw_b:

$$\sum_{j=1}^{N}\Bigg\{\left(B_iC_{ij}+\widetilde{B}_iA_{ij}+2\widetilde{B}_iB_{ij}\right)u_j+\left[\frac{1}{2}B_iA_{ij}\left(\sum_{k=1}^{N}C_{ik}w_{bk}\right)+\frac{1}{2}B_iA_{ij}\left(\sum_{k=1}^{N}C_{ik}w_{sk}\right)+\left(B_iB_{ij}+\widetilde{B}_iA_{ij}\right)\sum_{k=1}^{N}B_{ik}w_{bk}\right.$$
$$+\left(B_iB_{ij}+A_{ij}\widetilde{B}_i\right)\sum_{k=1}^{N}B_{ik}w_{sk}+\frac{1}{2}\left(B_iC_{ij}+A_{ij}\widetilde{B}_i+2B_{ij}\widetilde{B}_i\right)\sum_{k=1}^{N}A_{ik}w_{bk}+\frac{1}{2}\left(B_iC_{ij}+\widetilde{B}_iA_{ij}+2\widetilde{B}_iB_{ij}\right)\sum_{k=1}^{N}A_{ik}w_{sk}$$
$$+B_{ij}N_{xxi}+A_{ij}\widetilde{N}_{xxi}-D_iD_{ij}-2\widetilde{D}_iC_{ij}-\widetilde{D}_iB_{ij}+$$
$$\left.K_gB_{ij}-K_w\delta_{ij}-K_N\delta_{ij}(w_{bi})^2-2K_N\delta_{ij}w_{bi}w_{si}K_N\delta_{ij}(w_{si})^2\right]w_{bj}$$
$$\left[\frac{1}{2}B_iA_{ij}\left(\sum_{k=1}^{N}C_{ik}w_{bk}\right)+\frac{1}{2}B_iA_{ij}\left(\sum_{k=1}^{N}C_{ik}w_{sk}\right)+\left(B_iB_{ij}+\widetilde{B}_iA_{ij}\right)\sum_{k=1}^{N}B_{ik}w_{bk}+\left(B_iB_{ij}+\widetilde{B}_iA_{ij}\right)\sum_{k=1}^{N}B_{ik}w_{sk}+\right. \tag{43}$$
$$\frac{1}{2}\left(B_iC_{ij}+\widetilde{B}_iA_{ij}+2\widetilde{B}_iB_{ij}\right)\sum_{k=1}^{N}A_{ik}w_{bk}+\frac{1}{2}\left(B_iC_{ij}+\widetilde{B}_iA_{ij}+2\widetilde{B}_iB_{ij}\right)\sum_{k=1}^{N}A_{ik}w_{sk}+A_{ij}\widetilde{N}_{xxi}+B_{ij}N_{xxi}-D_{si}D_{ij}$$
$$\left.-2\widetilde{D}_{si}C_{ij}-\widetilde{D}_{si}B_{ij}+B_{ij}K_g-\delta_{ij}K_w-K_N\delta_{ij}(w_{bi})^2-2K_N\delta_{ij}w_{bi}w_{si}K_N\delta_{ij}(w_{si})^2\right]w_{sj}\Bigg\}$$
$$=\mathscr{I}_{1i}\sum_{j=1}^{N}A_{ij}\frac{d^2u_j}{dt^2}+\widetilde{\mathscr{I}}_{1i}\frac{d^2u_i}{dt^2}+\mathscr{I}_{0i}\frac{d^2w_{bi}}{dt^2}-\mathscr{I}_{2i}\sum_{j=1}^{N}B_{ij}\frac{d^2w_{bj}}{dt^2}-\widetilde{\mathscr{I}}_{2i}\sum_{j=1}^{N}A_{ij}\frac{d^2w_{bj}}{dt^2}$$
$$+\mathscr{I}_{0i}\frac{d^2w_{si}}{dt^2}-J_{2i}\sum_{j=1}^{N}B_{ij}\frac{d^2w_{sj}}{dt^2}-\widetilde{J}_{2i}\sum_{j=1}^{N}A_{ij}\frac{d^2w_{sj}}{dt^2}$$

δw_s:

$$\sum_{j=1}^{N}\Bigg\{\left(B_{si}C_{ij}+\widetilde{B}_{si}A_{ij}+2\widetilde{B}_{si}B_{ij}\right)u_j+\left[\frac{1}{2}B_{si}A_{ij}\left(\sum_{k=1}^{N}C_{ik}w_{bk}\right)+\frac{1}{2}B_{si}A_{ij}\left(\sum_{k=1}^{N}C_{ik}w_{sk}\right)+\left(B_{si}B_{ij}+\widetilde{B}_{si}A_{ij}\right)\sum_{k=1}^{N}B_{ik}w_{bk}\right.$$
$$+\left(B_{si}B_{ij}+\widetilde{B}_{si}A_{ij}\right)\sum_{k=1}^{N}B_{ik}w_{sk}+\frac{1}{2}\left(B_{si}C_{ij}+\widetilde{B}_{si}A_{ij}+2\widetilde{B}_{si}B_{ij}\right)\sum_{k=1}^{N}A_{ik}w_{bk}+\frac{1}{2}\left(B_{si}C_{ij}+\widetilde{B}_{si}A_{ij}+2\widetilde{B}_{si}B_{ij}\right)\sum_{k=1}^{N}A_{ik}w_{sk}$$
$$+B_{ij}N_{xxi}+A_{ij}\widetilde{N}_{xxi}-D_{si}D_{ij}-2\widetilde{D}_{si}C_{ij}-\widetilde{D}_{si}B_{ij}+$$
$$\left.K_gB_{ij}-K_w\delta_{ij}-K_N\delta_{ij}(w_{bi})^2-2K_N\delta_{ij}w_{bi}w_{si}K_N\delta_{ij}(w_{si})^2\right]w_{bj}+$$
$$\left[\frac{1}{2}B_{si}A_{ij}\left(\sum_{k=1}^{N}C_{ik}w_{bk}\right)+\frac{1}{2}B_{si}A_{ij}\left(\sum_{k=1}^{N}C_{ik}w_{sk}\right)+\left(B_{si}B_{ij}+\widetilde{B}_{si}A_{ij}\right)\sum_{k=1}^{N}B_{ik}w_{bk}+\left(B_{si}B_{ij}+\widetilde{B}_{si}A_{ij}\right)\sum_{k=1}^{N}B_{ik}w_{sk}+\right. \tag{44}$$
$$\frac{1}{2}\left(B_{si}C_{ij}+\widetilde{B}_{si}A_{ij}+2\widetilde{B}_{si}B_{ij}\right)\sum_{k=1}^{N}A_{ik}w_{bk}+\frac{1}{2}\left(B_{si}C_{ij}+\widetilde{B}_{si}A_{ij}+2\widetilde{B}_{si}B_{ij}\right)\sum_{k=1}^{N}A_{ik}w_{sk}+A_{ij}\widetilde{N}_{xxi}+B_{ij}N_{xxi}-H_{si}D_{ij}$$
$$\left.-2\widetilde{H}_{si}C_{ij}-\widetilde{H}_{si}B_{ij}+A_{si}B_{ij}+\widetilde{A}_{si}A_{ij}+B_{ij}K_g-\delta_{ij}K_w-K_N\delta_{ij}(w_{bi})^2-2K_N\delta_{ij}w_{bi}w_{si}K_N\delta_{ij}(w_{si})^2\right]w_{sj}\Bigg\}$$
$$=J_{1i}\sum_{j=1}^{N}A_{ij}\frac{d^2u_j}{dt^2}+\widetilde{J}_{1i}\frac{d^2u_i}{dt^2}+\mathscr{I}_{0i}\frac{d^2w_{bi}}{dt^2}-\widetilde{J}_{2i}\sum_{j=1}^{N}A_{ij}\frac{d^2w_{bj}}{dt^2}-J_{2i}\sum_{j=1}^{N}B_{ij}\frac{d^2w_{bj}}{dt^2}+\mathscr{I}_{0i}\frac{d^2w_{si}}{dt^2}-K_{2i}\sum_{j=1}^{N}B_{ij}\frac{d^2w_{sj}}{dt^2}$$
$$-\widetilde{K}_{2i}\sum_{j=1}^{N}A_{ij}\frac{d^2w_{sj}}{dt^2}$$

where:

$$\widetilde{\alpha}=\frac{d\alpha}{dx}\quad \text{for}(\alpha=A,A_s,B,B_s,D,D_s,H_s,\mathscr{I}_1,\mathscr{I}_2,J_1,J_2,K_2,N_{xx}) \tag{45}$$

$$N_{xxi}=\sum_{j=1}^{N}\left\{A_iA_{ij}u_j+\left(\frac{1}{2}A_iA_{ij}\sum_{k=1}^{N}A_{ik}w_{sk}+\frac{1}{2}A_iA_{ij}\sum_{k=1}^{N}A_{ik}w_{bk}-B_iB_{ij}\right)w_{bj}+\left(\frac{1}{2}A_iA_{ij}\sum_{k=1}^{N}A_{ik}w_{bk}+\frac{1}{2}A_iA_{ij}\sum_{k=1}^{N}A_{ik}w_{sk}-B_{si}B_{ij}\right)w_{sj}\right\} \tag{46}$$

The end conditions discretized form is shown as Eqs. (47)–(50)

$$u=0\quad\text{or}\quad\sum_{j=1}^{N}\Bigg\{A_iA_{ij}u_j+\left(\frac{1}{2}A_iA_{ij}\sum_{k=1}^{N}A_{ik}w_{bk}+\frac{1}{2}A_iA_{ij}\sum_{k=1}^{N}A_{ik}w_{sk}-B_iB_{ij}\right)w_{bj}$$
$$+\left(\frac{1}{2}A_iA_{ij}\sum_{k=1}^{N}A_{ik}w_{bk}+\frac{1}{2}A_iA_{ij}\sum_{k=1}^{N}A_{ik}w_{sk}-B_{ij}B_{si}\right)w_{sj}\Bigg\}=0 \tag{47}$$

$$
\begin{aligned}
w_b = 0 \quad \text{or} \quad & \sum_{j=1}^{N}\Bigg\{ u_j\left(B_i B_{ij} + A_{ij}\widetilde{B}_i\right) + \left(\frac{1}{2}\left(\sum_{k=1}^{N} B_{ik} w_{bk}\right) A_{ij} B_i + \frac{1}{2}\left(\sum_{k=1}^{N} B_{ik} w_{sk}\right) A_{ij} B_i \right. \\
& + \frac{1}{2}\left(\sum_{k=1}^{N} A_{ik} w_{bk}\right) B_i B_{ij} + \frac{1}{2}\left(\sum_{k=1}^{N} A_{ik} w_{sk}\right) B_i B_{ij} - C_{ij} D_i + A_{ij} N_{xxi} \\
& + A_{ij} K_g + \frac{1}{2}\left(\sum_{k=1}^{N} A_{ik} w_{bk}\right) A_{ij}\widetilde{B}_i + \frac{1}{2}\left(\sum_{k=1}^{N} A_{ik} w_{sk}\right) A_{ij}\widetilde{B}_i - B_{ij}\widetilde{D}_i \Bigg) w_{bj} \\
& + \left(\frac{1}{2}\left(\sum_{k=1}^{N} B_{ik} w_{bk}\right) A_{ij} B_i + \frac{1}{2}\left(\sum_{k=1}^{N} B_{ik} w_{sk}\right) A_{ij} B_i + \frac{1}{2}\left(\sum_{k=1}^{N} A_{ik} w_{bk}\right) B_i B_{ij} \right. \\
& + \frac{1}{2}\left(\sum_{k=1}^{N} A_{ik} w_{sk}\right) B_i B_{ij} - C_{ij} D_{si} + A_{ij} N_{xxi} + A_{ij} K_g + \frac{1}{2}\left(\sum_{k=1}^{N} A_{ik} w_{bk}\right) A_{ij}\widetilde{B}_i \\
& \left. + \frac{1}{2}\left(\sum_{k=1}^{N} A_{ik} w_{sk}\right) A_{ij}\widetilde{B}_i - B_{ij}\widetilde{D}_{si}\right) w_{sj} \Bigg\} = \mathscr{I}_{1i} \sum_{j=1}^{N} A_{ij} \frac{d^2 u_j}{dt^2} - \mathscr{I}_{2i} \sum_{j=1}^{N} B_{ij} \frac{d^2 w_{bj}}{dt^2} \\
& - J_{2i} \sum_{j=1}^{N} B_{ij} \frac{d^2 w_{sj}}{dt^2}
\end{aligned} \tag{48}
$$

$$
\begin{aligned}
w_s = 0 \quad \text{or} \quad & \sum_{j=1}^{N}\Bigg\{ u_j\left(B_{ij} B_{si} + A_{ij}\widetilde{B}_{si}\right) + \left(\frac{1}{2}\left(\sum_{k=1}^{N} B_{ik} w_{bk}\right) A_{ij} B_{si} + \frac{1}{2}\left(\sum_{k=1}^{N} B_{ik} w_{sk}\right) A_{ij} B_{si} + \right. \\
& \frac{1}{2}\left(\sum_{k=1}^{N} A_{ik} w_{bk}\right) B_{ij} B_{si} + \frac{1}{2}\left(\sum_{k=1}^{N} A_{ik} w_{sk}\right) B_{ij} B_{si} - C_{ij} D_{si} + A_{ij} N_{xxi} + A_{ij} K_g + \\
& \frac{1}{2}\left(\sum_{k=1}^{N} A_{ik} w_{bk}\right) A_{ij}\widetilde{B}_{si} + \frac{1}{2}\left(\sum_{k=1}^{N} A_{ik} w_{sk}\right) A_{ij}\widetilde{B}_{si} - B_{ij}\widetilde{D}_{si}\Bigg) w_{bj} + \\
& \left(A_{si} A_{ij} + \frac{1}{2}\left(\sum_{k=1}^{N} B_{ik} w_{bk}\right) A_{ij} B_{si} + \frac{1}{2}\left(\sum_{k=1}^{N} B_{ik} w_{sk}\right) A_{ij} B_{si} + \frac{1}{2}\left(\sum_{k=1}^{N} A_{ik} w_{bk}\right) B_{ij} B_{si} \right. \\
& + \frac{1}{2}\left(\sum_{k=1}^{N} A_{ik} w_{sk}\right) B_{ij} B_{si} + A_{ij} N_{xxi} + A_{ij} K_g + \frac{1}{2}\left(\sum_{k=1}^{N} A_{ik} w_{bk}\right) A_{ij}\widetilde{B}_{si} + \\
& \left. \frac{1}{2}\left(\sum_{k=1}^{N} A_{ik} w_{sk}\right) A_{ij}\widetilde{B}_{si} - B_{ij}\widetilde{H}_{si} - C_{ij} H_{si}\right) w_{sj} \Bigg\} = J_{1i} \sum_{j=1}^{N} A_{ij} \frac{d^2 u_j}{dt^2} - J_{2i} \sum_{j=1}^{N} B_{ij} \frac{d^2 w_{bj}}{dt^2} \\
& - K_{2i} \sum_{j=1}^{N} B_{ij} \frac{d^2 w_{sj}}{dt^2}
\end{aligned} \tag{49}
$$

$$
\begin{aligned}
& \frac{\partial w_b}{\partial x} = 0 \quad \text{or} \quad \sum_{j=1}^{N}\Bigg\{ A_{ij} B_i u_j + \left(\frac{1}{2} B_i A_{ij} \sum_{k=1}^{N} A_{ik} w_{bk} + \frac{1}{2} A_{ij} B_i \sum_{k=1}^{N} A_{ik} w_{sk} - B_{ij} D_i\right) w_{bj} \\
& + \left(\frac{1}{2} A_{ij} B_i \sum_{k=1}^{N} A_{ik} w_{bk} + \frac{1}{2} A_{ij} B_i \sum_{k=1}^{N} A_{ik} w_{sk} - B_{ij} D_{si}\right) w_{sj} \Bigg\} = 0 \\
& \frac{\partial w_s}{\partial x} = 0 \quad \text{or} \quad \sum_{j=1}^{N}\Bigg\{ A_{ij} B_{si} u_j + \left(\frac{1}{2} A_{ij} B_{si} \sum_{k=1}^{N} A_{ik} w_{bk} + \frac{1}{2} A_{ij} B_{si} \sum_{k=1}^{N} A_{ik} w_{sk} - B_{ij} D_{si}\right) w_{bj} \\
& + w_{sj}\left(\frac{1}{2} A_{ij} B_{si} \sum_{k=1}^{N} A_{ik} w_{bk} + \frac{1}{2} A_{ij} B_{si} \sum_{k=1}^{N} A_{ik} w_{sk} - B_{ij} H_{si}\right)\Bigg\} = 0
\end{aligned} \tag{50}
$$

Eqs. (42)–(44) and associated boundary conditions can be stated in the matrix form as Eq. (51) [33,35], which reduces them to an eigenvalue problem.

$$(K_L + K_{NL})d + M\ddot{d} = 0 \tag{51}$$

the linear and nonlinear stiffness matrixes, respectively, are K_L and K_{NL}. The mass matrix M.

The unidentified vector $d = \{\{\bar{u}\}, \{\bar{w}_b\}, \{\bar{w}_s\}\}^T$ in where d stands for domain points.

The unidentified vector $b = \{\{\bar{u}\}, \{\bar{w}_b\}, \{\bar{w}_s\}\}^T$ where b stands for boundary points.

The harmonic form is presumed for free vibration analysis Eq. (52), so [33,35]:

$$d = d_0 e^{i\omega t}, u = \bar{u} e^{i\omega t}, w_b = \bar{w}_b e^{i\omega t}, w_s = \bar{w}_s e^{i\omega t} \tag{52}$$

Table 1
Material properties [37].

	E (GPa)	ρ (kg /m^3)	υ
Tungsten (W)	411	19,250	0.3
Copper (CU)	120	8960	0.3

where ω is the natural frequency without dimensions. The unidentified coefficient (d_0) is connected to various displacement components.

Eq. (52) is substituted into Eq. (51) to produce Eqs. (53) and (54) [33,35,47].

$$\left(K_L + K_{NL} - \omega^2 M\right) d_0 = 0 \tag{53}$$

$$\begin{bmatrix} M_{bb} & 0 \\ 0 & M_{dd} \end{bmatrix} \begin{Bmatrix} d_b^{\cdot\cdot} \\ d_d^{\cdot\cdot} \end{Bmatrix} + \begin{bmatrix} K_{bb}^{L} + K_{bb}^{NL} & K_{bd} \\ K_{db} & K_{dd} \end{bmatrix} \begin{Bmatrix} d_b \\ d_d \end{Bmatrix} = \{0\} \tag{54}$$

Malekzadeh explained how to use the harmonic balancing approach, and this results in Eq. (55) [33,35,47]:

$$\begin{bmatrix} K_{bb}^{L} + \frac{3}{4} K_{bb}^{NL} & K_{bd} \\ K_{db} & K_{dd} \end{bmatrix} \begin{Bmatrix} d_b \\ d_d \end{Bmatrix} - \omega^2 \begin{bmatrix} M_{bb} & 0 \\ 0 & M_{dd} \end{bmatrix} \begin{Bmatrix} d_b \\ d_d \end{Bmatrix} = \{0\} \tag{55}$$

Considering the defined displacements for 3 N unknowns (N is the number of discrete points), and taking into account the boundary conditions for a simple supported beam, the number of unknowns and consequently the required number of equations is reduced to 10 equations out of the total number of equations (two conditions for longitudinal displacement, four conditions for transverse displacement including bending and shear, and four conditions for moments).

Where M dimension is (3N-10) × (3N-10) and M matrix is the mass matrix, and the dimension of K_{bb} is 10 × 10 matrix, K_{db} is 10 × (3N-10) matrix, and K_{bd} is 10 × (3N-10) matrix, respectively.

Equation (55) is a nonlinear eigenvalue problem, which means that it cannot be addressed using standard techniques that rely on linear solutions. The nonlinear constitutive equations are solved in this work using an iterative method. The following stages are taken during the operation [33,35,47]:

Step 1. From Eq. (55), a linear frequency ω_L and its corresponding eigenvector are derived without taking into account the nonlinear component k_{NL}.

Step 2. A new eigenvalue and its corresponding eigenvector can be extracted by doing k_{NL} calculations using the acquired eigenvector.

This step involves normalizing the eigenvectors linked to the eigenvalues of Eq. (55) concerning the deflection of the corresponding FG beam section (x_m). These vectors are then created by multiplying them by the factor (W_m /r). W_m is a value representing the transverse displacement of section $x = x_m$ and $r = \sqrt{bh^3/12A}$ is the radius of cross-sectional gyration.

Step 3. The iterative process is repeated until the nonlinear frequency from the two international consecutive stages equal 0.0001 for a particular value (W_m /r). then ω_{NL}, a nonlinear frequency is attained.

3. Numerical results and discussion

Ensure that the results are accurate by comparing them with other solutions. In nonlinear vibration states, a bi-directional beam is proposed consisting of Tungsten (W) in the top layer and Copper (Cu) in the bottom layer. Therefore, using the suggested formulations for FG beams exposed to various boundary conditions, it is necessary to examine convergence behavior and correctness. In Table 1 [37], these materials are listed according to their properties.

It is stated as the non-dimensional frequency parameter Eq. (56)

$$\lambda_n = \frac{\omega_n L^2}{h} \sqrt{\frac{\rho_m}{E_m}} \tag{56}$$

where ρ_m and E_m stand for the metallic part's density and Young's modulus, respectively.

Additionally, the numerical findings are provided as the elastic substrate constants utilized in equations. Eq. (57)

$$K_w = \frac{k_w L^4}{E_m I}, K_g = \frac{k_g L^2}{\pi^2 E_m I} \tag{57}$$

where I is considered as Eq. (58)

Table 2
Convergence of the frequency ratio $\lambda_i = \omega_{NL}/\omega_L$ (RBT) for simply supported Bi-di beam ($K_w = K_g = 0$, $e_0 = 0$, $p_z = 2$, $\omega_{max}/r = 0.5$).

L/h		Number of grid points N_x					
5	Nmode	7	9	11	13	15	17
	1	1.101	1.1118	0.9725	0.9725	0.9725	0.9724
	2	1.0602	1.0502	1.0517	1.0517	1.0517	1.0517
	3	1.0021	0.8454	0.8659	0.8229	0.8229	0.8228
10	1	0.9588	0.9700	1.1089	0.9691	0.9691	0.9690
	2	1.0626	1.0429	1.0459	1.0460	1.0462	1.0461
	3	1.0411	1.0526	1.0801	1.0736	1.0736	1.07464

Table 3
Convergence of the frequency ratio $\lambda_i = \omega_{NL}/\omega_L$ (RBT) for clamped-clamped Bi-di beam ($K_w = K_g = 0$, $e_0 = 0$, $p_x = 2$, $\omega_{max}/r = 0.4$).

L/h		Number of grid points N_x					
5	Nmode	7	9	11	13	15	17
	1	0.9899	1.00362	1.0133	1.0133	1.0134	1.0144
	2	1.0116	1.0109	1.0187	1.0188	1.0187	1.0189
	3	1.00701	1.0792	1.0793	1.0793	1.0792	1.0791
10	1	1.00536	1.0099	1.0097	1.0055	1.00554	1.0055
	2	1.00129	1.00137	1.00139	1.00232	1.00232	1.00231
	3	1.00229	1.00301	1.00369	1.00315	1.00315	1.00313

Table 4
Difference of frequency ratios $\lambda_i = \omega_{NL}/\omega_L$ between EBT, TBT [33], and current study (RBT) for isotropic FG beam.

	Wm/r = 1			Wm/r = 2			Wm/r = 3		
	EBT	TBT	RBT (Present)	EBT	TBT	RBT (Present)	EBT	TBT	RBT (Present)
C–C (λ_1)	1.0222	1.0240	1.0357	1.0858	1.0939	1.1352	1.1833	1.2048	1.2818
C–C (λ_2)	1.0485	1.0630	1.0854	1.1793	1.2505	1.2986	1.3636	1.5987	1.5715
S–C (λ_1)	1.0641	1.0653	1.0809	1.2319	1.2376	1.2820	1.4605	1.4767	1.5371

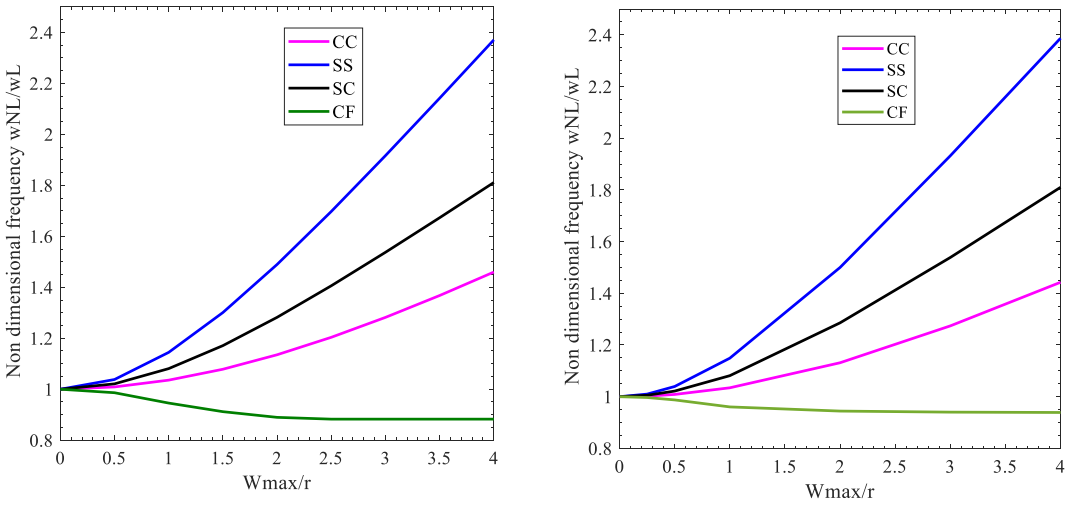

Fig. 2. The influence of various end conditions on Nonlinear-to-linear parameter ω_{NL}/ω_L for the isotropic beam for L/h = 100, L/h = 8 in respect of various amplitude ratio ω_{max}/r.

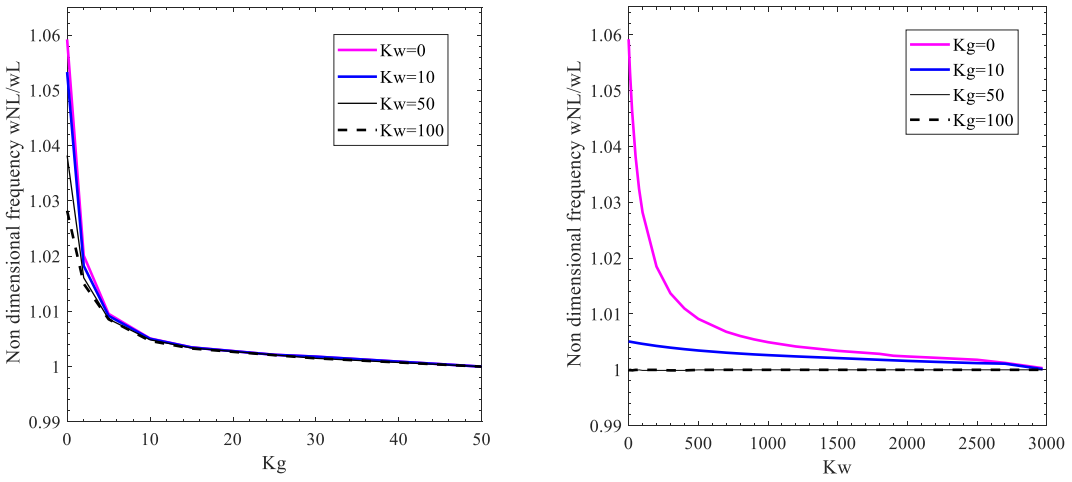

(a) Effect of the stiffness K_w on ω_{NL}/ω_L (b) Effect of the stiffness K_g on ω_{NL}/ω_L

Fig. 3. Effect of the substrate stiffness K_w and K_g on nonlinear to linear parameter of SS isotropic beam ($l/h = 5$, $\omega_{max}/r = 0.6$).

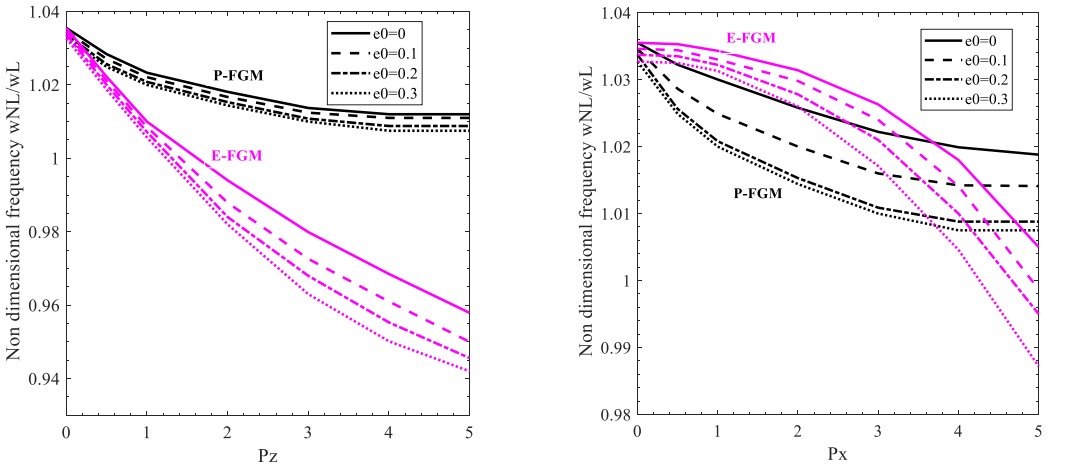

(a) the effect of porosity and pz on ω_{NL}/ω_L (b) the effect of porosity and px on ω_{NL}/ω_L

Fig. 4. Nonlinear to linear frequency parameter altering of C–C porous beams in respect of power law indexes pz, px for various porosity coefficients ($l/h = 5$, $\omega_{max}/r = 1$).

$$I = \frac{bh^3}{12} \tag{58}$$

In each scenario, the nonlinear to linear frequency ratio of the bi-directional FG beam concerning the quantity of DQ grid points along x direction is investigated first. Under simple support conditions and clamped-clamped supported end conditions, the nonlinear to linear convergence behavior of bi-directional FG beams is shown in Tables 2 and 3 for three modes. With $Nx = 13$, converged results are obtained.

Nonlinear to linear frequency ratios $\lambda = \omega_{NL}/\omega_L$ of beams with CC and CS end conditions are shown in Table 4. A comparison is made between the results of Malekzadeh and Shojaee [33] based on EBT and TBT. A strong agreement can be seen between the current work (RBT) and the previous techniques. It is observed that the lowest frequency ratio is related to the Clamp-Clamp support and the highest one is related to the Clamp-Simply support. It should be noted that although it was expected that the highest frequency ratio would be related to the CC support, due to the geometry of the supports and the lack of geometric symmetry in the CS support, the highest frequency ratio is observed for this type of support.

In Fig. 1, The Sketch of bi-directional FG beam lying on substrate is illustrated. The frequency ratios $\lambda = \omega_{NL}/\omega_L$ between nonlinear

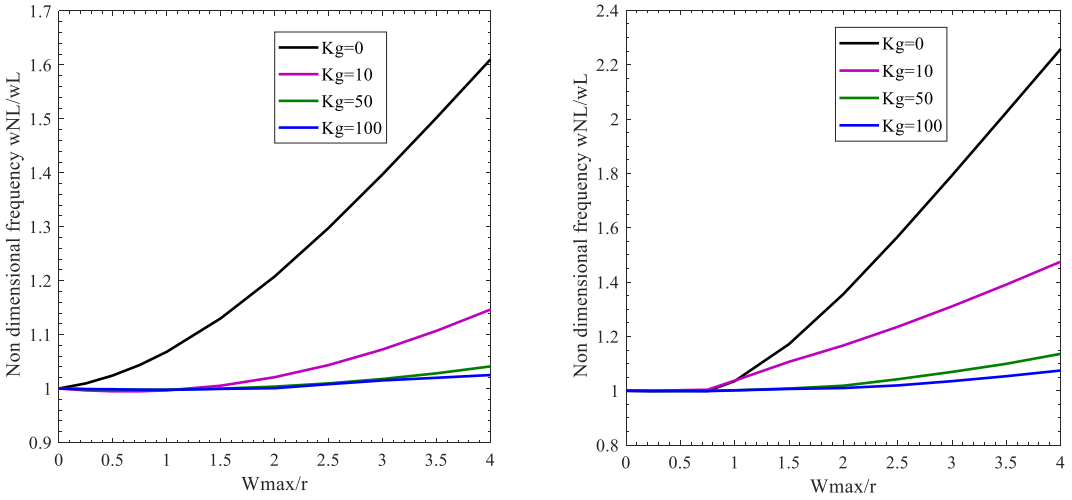

Fig. 5. Impact of the shear substrate stiffness K_g on the nonlinear to linear frequency of the CC and SS FG beams concerning various values of the amplitude ratio ω_{max}/r (l/h = 5, Pz = 2).

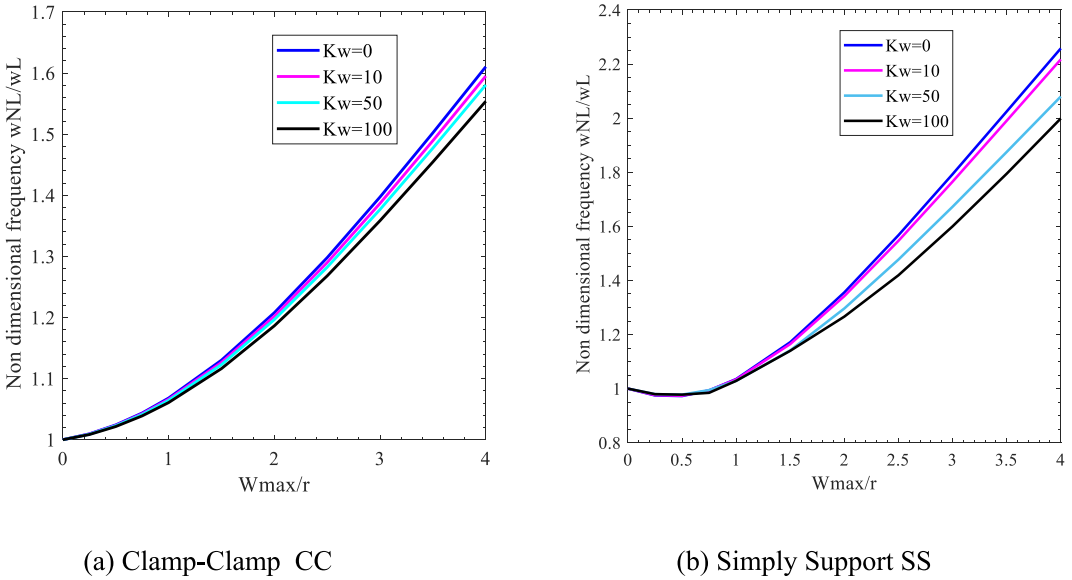

Fig. 6. The influence of Winkler substrate stiffness K_w on the nonlinear to linear frequennncy of the CC and SS FG beams concerning various values of the amplitude ratio ω_{max}/r (l/h = 5, Pz = 2).

and linear isotropic beams with various end conditions are shown in Fig. 2(a and b) via various amplitude ratios ω_{max}/r for L/h = 100 and L/h = 8 respectively. One of the important features of this analysis is the investigsation of vibration frequencies versus amplitude ratios, which is well shown in this dependence curve. Whereas amplitude ratios less than 0.5 the slope of the graph of non-linear frequency changes is very low, and in the range of 0.5–2, the trend of changes is increasing with a steep slope and this trend continues with a constant slope in the end. A clamped-free end assumption has the least tendency to affect frequency ratio, while simply supported end conditions have the greatest tendency. In addition, the ratio of nonlinear to linear frequency is found to be significantly impacted by the soar of amplitude ratio values.

In Fig. 3(a and b), variation of amplitude ratios under K_w and K_g are shown respectively for nonlinear to linear frequency of isotropic beams with different boundary conditions. When an end condition is clamped-free, the frequency ratio is the least likely to be affected, whereas when it is simply supported, the frequency ratios under K_w and K_g is most likely to be affected. Furthermore, an increase in shear stiffness of the substrate K_g values significantly impact the ratio of nonlinear to linear parameter.

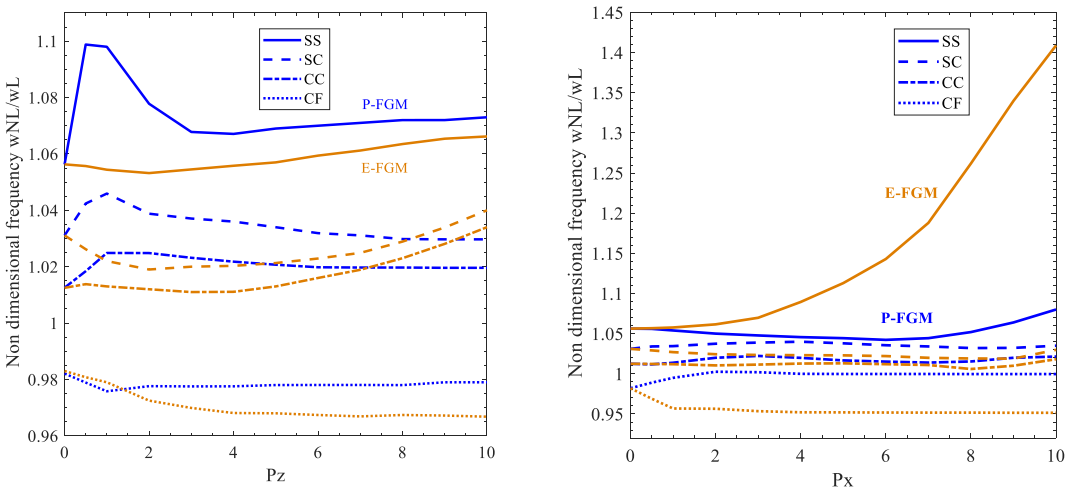

Fig. 7. Various end conditions influence on nonlinear to linear parameter ω_{NL}/ω_L of the Bidirectional FG beam versus power law indexes pz, px (l/h = 8, ω_{max}/r = 0.6).

In Fig. 4(a and b), the growth of porosity coefficients is examined in relation to the nonlinear to linear frequency parameter of a bi-dimensional beam for both power-law and exponential FG different indexes pz, px. A gradual decline in the nonlinear to linear parameter is evident as each pz or px increases. Therefore, increasing porosity coefficients result in a substantial fall in frequency ratios. So, by increasing the porosity coefficient and material gradient in two directions, the frequency ratio decreases significantly due to the decrease in beam stiffness. The difference between exponential and power-law model frequencies can be seen by comparing the figures. This difference is due to the difference in the changes of material properties with the increase of the gradient of material properties in the two models; So that with the soar of material gradient in two directions, the rate of change of material properties in the exponential model is higher and the reduction of the beam stiffness is more severe and as a result, the decrease of the dimensionless nonlinear frequency is more severe in the exponential model.

CC and SS end conditions are shown in Fig. 5(a and b) respectively, along with different amplitude ratios ω_{max}/r for different shear substrate stiffness K_g for l/h = 5 and pz = 2. There is no doubt that raising the deflection ratio values causes the frequency ratio to grow for both clamped and simply supported FG beams. SS beams, though have a more abrupt rise than clamped beams. Moreover, as the magnitude of the shear substrate stiffness K_g increases, the nonlinear to linear parameter noticeably decrease. Due to the increased stiffness of the shear substrate K_g, the beam's total stiffness increase

Fig. 6(a and b) show how the Winkler substrate stiffness K_w affects the nonlinear to linear frequency of the CC and SS FG beams concerning various ω_{max}/r values for the amplitude rising. As can be observed, the frequency parameter steadily decreases as Winkler substrate stiffness increases to raise FG beam stiffness. The thing is, FG beam stiffness having a greater impact on linear frequency than nonlinear frequency. Additionally, the frequency parameters are smaller under higher Winkler substrate ratios stiffness K_w than they are under lower stiffness, and the disparity between these tendencies increases at higher amplitude ω_{max}/r. In addition, the soar in the coefficient of the Winkler elastic substrate leads to a decline in the ratio of the nonlinear frequency to the linear for all boundary conditions. It should be mentioned that the presence of the linear elastic substrate causes a climb in the stiffness of the beam and ultimately a soar in the linear and non-linear frequencies, But a linear frequency increase is greater than a non-linear one.

In Fig. 7(a and b), the trend of nonlinear to linear parameter changing via material gradients pz, px is given for both power-law and exponential bi-directional FG beams. It is evident that for the gradual increase of material gradients in each direction the frequency ratio mostly drops but it does not follow the same trend for each boundary condition except for E-FGM in the SS end condition. It should also be noted that when the gradient of the properties of the material in z direction is reduced below the number one, the frequency ratio increases, which is due to the increase in the stiffness of the beam in this range, and the index number of the gradient one in the z direction is the turning point of this change.

4. Conclusion

The nonlinear frequency of a bi-directional porous functionally graded beam is evaluated in this study utilizing third-order shear deformation theory, Green's tensor, and von Karman geometric nonlinearity. In this situation, Hamilton's principle is applied to construct constitutive equations and end conditions. A precise and efficient numerical methodology, the generalized differential quadrature method (GDQM) uses a direct iteration approach to solve discretized nonlinear equations. The FGM material model, vibration amplitude ratios, material indices, elastic substrate parameters, porosity coefficient, and various boundary conditions are all

evaluated to confirm the results. Based on the findings, the following conclusions were reached:

1) The ratio of nonlinear to linear frequency to amplitude increases depending on the type of end condition; however, this trend does not exist for C–F endpoints.
2) The nonlinear to linear frequency ratio fluctuates with the z and x material gradients.
3) The influence of porosity coefficients, power law, and material indexes increases as the nonlinear to linear frequency ratio decreases due to the stiffness of bi-directional FG beams decreasing.
4) The frequency ratio under porosity influences tends to be more influenced by the power-law index along the x-orientation than by the power-law index in the z-orientation.
5) How an isotropic beam's nonlinear to linear frequency ratio is impacted by the altering K_w and K_g substrate stiffness.
6) Study examines nonlinear to linear frequency ratios as a function of amplitude ratios by varying the FG beam's Shear and Winkler substrate stiffness and comparing their trends.

Author contribution statement

Mohammadamin Forghani: Conceived and designed the analysis; Wrote the paper.
Yousef Bazarganlari: Contributed analysis tools or data; Wrote the paper.
Parham Zahedinejad: Conceived and designed the data; Analyzed and interpreted the data.
Mohammad Javad Kazemzadeh-Parsi: Analyzed and interpreted the data; Wrote the paper.

Data availability statement

Data will be made available on request.

Declaration of competing interest

The authors declare that they have no known competing financial interests or personal relationships that could have appeared to influence the work reported in this paper.

References

[1] P. Zahedinejad, Free vibration analysis of functionally graded beams resting on elastic foundation in thermal environment, Int. J. Struct. Stabil. Dyn. 16 (7) (2016), 1550029, https://doi.org/10.1142/S0219455415500297.
[2] Y. Wen, Q.Y. Zeng, A high-order finite element formulation for vibration analysis of beam-type structures, 460, Int. J. Struct. Stabil. Dyn. 9 (4) (2009) 649, https://doi.org/10.1142/S0219455409003223.
[3] M. Aydogdu, V. Taskin, Free vibration analysis of functionally graded beams with simply supported edges, Mater. Des. 28 (5) (2007) 1651–1656, https://doi.org/10.1016/j.matdes.2006.02.007.
[4] M. Simsek, Fundamental frequency analysis of functionally graded beams by using different higher-order beam theories, Nucl. Eng. Des. 240 (4) (2010) 697–705, https://doi.org/10.1016/j.nucengdes.2009.12.013.
[5] H.T. Thai, T.P. Vo, Bending and free vibration of functionally graded beams using various higher-order shear deformation beam theories, Int. J. Mech. Sci. 62 (1) (2012) 57–66, https://doi.org/10.1016/j.ijmecsci.2012.05.014.
[6] S. Chakraverty, K.K. Pradhan, Free vibration of exponential functionally graded rectangular plates in thermal environment with general boundary conditions, Aero. Sci. Technol. 36 (2014) 132–156, https://doi.org/10.1016/j.ast.2014.04.005.
[7] N. Wattanasakulpong, A. Chaikittiratana, S. Pornpeerakeat, Chebyshev collocation approach for vibration analysis of functionally graded porous beams based on third-order shear deformation theory, Acta Mech. Sin. 34 (6) (2018) 1124–1135, https://doi.org/10.1007/s10409-018-0770-3.
[8] Y. Wang, H. Ma, K. Xie, et al., Nonlinear bending of a sandwich beam with metal foam and GPLRC face-sheets using Chebyshev–Ritz method, Thin-Walled Struct. 181 (2022), 110035, https://doi.org/10.1016/j.tws.2022.110035.
[9] W. Zhang, C. Wang, Y. Wang, Thermo-mechanical analysis of porous functionally graded graphene reinforced cylindrical panels using an improved third order shear deformable model, Appl. Math. Model. 118 (2023) 453–473, https://doi.org/10.1016/j.apm.2023.01.026.
[10] D. Zhou, A general solution to vibrations of beams on variable Winkler elastic foundation, Comput. Struct. 47 (1) (1993) 83–90, https://doi.org/10.1016/0045-7949(93)90281-H.
[11] M. Eisenberger, Vibration frequencies for beams on variable one-and two-parameter elastic foundations, J. Sound Vib. 176 (5) (1994) 577–584, https://doi.org/10.1006/jsvi.1994.1399.
[12] S.C. Pradhan, T. Murmu, Thermo-mechanical vibration of FGM sandwich beam under variable elastic foundations using differential quadrature method, J. Sound Vib. 321 (1–2) (2009) 342–362, https://doi.org/10.1016/j.jsv.2008.09.018.
[13] P. Malekzadeh, G. Karami, A mixed differential quadrature and finite element free vibration and buckling analysis of thick beams on two-parameter elastic foundations, Appl. Math. Model. 32 (7) (2008) 1381–1394, https://doi.org/10.1016/j.apm.2007.04.019.
[14] S.D. Akbas, Free vibration and bending of functionally graded beams resting on elastic foundation, Res. Eng. Struct. Mater. 1 (1) (2015) 25–37, https://doi.org/10.17515/resm2015.03st0107.
[15] M.H. Yas, S. Kamarian, A. Pourasghar, Free vibration analysis of functionally graded beams resting on variable elastic foundations using a generalized power-law distribution and GDQ method, Ann. Solid Struct. Mech. 9 (1) (2017) 1–11, https://doi.org/10.1007/s12356-017-0046-9.
[16] P. Tossapanon, N. Wattanasakulpong, Stability and free vibration of functionally graded sandwich beams resting on two-parameter elastic foundation, Compos. Struct. 142 (2016) 215–225, https://doi.org/10.1016/j.compstruct.2016.01.085.
[17] L. Li, X. Li, Y. Hu, Nonlinear bending of a two-dimensionally functionally graded beam, Compos. Struct. 184 (2018) 1049–1061, https://doi.org/10.1016/j.compstruct.2017.10.087.
[18] J. Lei, Y. He, Z. Li, S. Guo, D. Liu, Post buckling analysis of bi-directional functionally graded imperfect beams based on a novel third-order shear deformation theory, Compos. Struct. 209 (2019) 811–829, https://doi.org/10.1016/j.compstruct.2018.10.106.
[19] M. Simsek, Bi-directional functionally graded materials (BDFGMs) for free and forced vibration of Timoshenko beams with various boundary conditions, Compos. Struct. 133 (2015) 968–978, https://doi.org/10.1016/j.compstruct.2015.08.021.

[20] Z.H. Wang, X.H. Wang, G.D. Xu, S. Cheng, T. Zeng, Free vibration of two-directional functionally graded beams, Compos. Struct. 135 (2016) 191–198, https://doi.org/10.1016/j.compstruct.2015.09.013.
[21] A. Ghorbanpour Arani, S. Niknejad, Dynamic stability analysis of Bi-directional functionally graded beam with various shear deformation theories under harmonic excitation and thermal environment, J. Solid Mech. (2020), https://doi.org/10.22034/jsm.2020.678358.
[22] M.J. Kazemzadeh-Parsi, C. Francisco, A. Amine, Proper generalized decomposition for parametric study and material distribution design of multi-directional functionally graded plates based on 3D elasticity solution, Materials 14 (21) (2021) 6660, https://doi.org/10.3390/ma14216660.
[23] N. Wattanasakulpong, A. Chaikittiratana, Flexural vibration of imperfect functionally graded beams based on Timoshenko beam theory: Chebyshev collocation method, Meccanica 50 (5) (2015) 1331–1342, https://doi.org/10.1007/s11012-014-0094-8.
[24] J. Zhu, Z. Lai, Z. Yin, J. Jeon, S. Lee, Fabrication of ZrO2–NiCr functionally graded material by powder metallurgy, Mater. Chem. Phys. 68 (1–3) (2001) 130–135, https://doi.org/10.1016/S0254-0584(00)00355-2.
[25] D. Chen, J. Yang, S. Kitipornchai, Free and forced vibrations of shear deformable functionally graded porous beams, Int. J. Mech. Sci. 108 (2016) 14–22, https://doi.org/10.1016/j.ijmecsci.2016.01.025.
[26] Y.S. Al Rjoub, A.G. Hamad, Free vibration of functionally Euler-Bernoulli and Timoshenko graded porous beams using the transfer matrix method, KSCE J. Civil Eng. 21 (3) (2017) 792–806, https://doi.org/10.1007/s12205-016-0149-6.
[27] N. Shafiei, S.S. Mirjavadi, B. MohaselAfshari, S. Rabby, M. Kazemi, Vibration of two-dimensional imperfect functionally graded (2D-FG) porous nano-/micro-beams, Comput. Methods Appl. Mech. Eng. 322 (2017) 615–632, https://doi.org/10.1016/j.cma.2017.05.007.
[28] F. Ebrahimi, A. Jafari, A higher-order thermomechanical vibration analysis of temperature-dependent FGM beams with porosities, J. Eng. (2016), https://doi.org/10.1155/2016/9561504.
[29] N. Wattanasakulpong, A. Chaikittiratana, S. Pornpeerakeat, Chebyshev collocation approach for vibration analysis of functionally graded porous beams based on third-order shear deformation theory, Acta Mech. Sin. 34 (6) (2018) 1124–1135, https://doi.org/10.1007/s10409-018-0770-3.
[30] F. Ebrahimi, M. Zia, Large amplitude nonlinear vibration analysis of functionally graded Timoshenko beams with porosities, Acta Astronaut. 116 (2015) 117–125, https://doi.org/10.1016/j.actaastro.2015.06.014.
[31] M. Khakpour, Y. Bazargan-Lari, P. Zahedinejad, M.J. Kazemzadeh-Parsi, Vibrations evaluation of functionally graded porous beams in thermal surroundings by generalized differential quadrature method, Shock Vib. (2022) 2022, https://doi.org/10.1155/2022/8516971.
[32] S. Kitipornchai, L.L. Ke, J. Yang, Y. Xiang, Nonlinear vibration of edge cracked functionally graded Timoshenko beams, J. Sound Vib. 324 (3–5) (2009) 962–982, https://doi.org/10.1016/j.jsv.2009.02.023.
[33] P. Malekzadeh, M. Shojaee, Surface and nonlocal effects on the nonlinear free vibration of non-uniform nanobeams, Compos. B Eng. 52 (2013) 84–92, https://doi.org/10.1016/j.compositesb.2013.03.046.
[34] N. Wattanasakulpong, A. Chaikittiratana, On the linear and nonlinear vibration responses of elastically end restrained beams using DTM, Mech. Base. Des. Struct. Mach. 42 (2) (2014) 135–150. http://www.tandfonline.com/loi/lmbd20.
[35] T. Yang, Y. Tang, Q. Li, X.D. Yang, Nonlinear bending, buckling and vibration of bi-directional functionally graded nanobeams, Compos. Struct. 204 (2018) 313–319, https://doi.org/10.1016/j.compstruct.2018.07.045.
[36] M.H. Ghayesh, Nonlinear vibration analysis of axially functionally graded shear-deformable tapered beams, Appl. Math. Model. 59 (2018) 583–596, https://doi.org/10.1016/j.apm.2018.02.017.
[37] K. Xie, Y. Wang, X. Fan, T. Fu, Nonlinear free vibration analysis of functionally graded beams by using different shear deformation theories, Appl. Math. Model. 77 (2020) 1860–1880, https://doi.org/10.1016/j.apm.2019.09.024.
[38] W. Songsuwan, N. Wattanasakulpong, T.P. Vo, Nonlinear vibration of third-order shear deformable FG-GPLRC beams under time-dependent forces: Gram–Schmidt–Ritz method, Thin-Walled Struct. 176 (2022), 109343, https://doi.org/10.1016/j.tws.2022.109343.
[39] W. Songsuwan, N. Wattanasakulpong, S. Kumar, Nonlinear transient response of sandwich beams with functionally graded porous core under moving load, Eng. Anal. Bound. Elem. 155 (2023) 11–24, https://doi.org/10.1016/j.enganabound.2023.05.055.
[40] R. Bellman, B.G. Kashef, J. Casti, Differential quadrature: a technique for the rapid solution of nonlinear partial differential equations, J. Comput. Phys. 10 (1) (1972) 40–52, https://doi.org/10.1016/0021-9991(72)90089-7.
[41] W. Charles Bert, M. Malik, Differential Quadrature Method in Computational Mechanics: A Review, 1996, pp. 1–28, https://doi.org/10.1115/1.3101882.
[42] W. Chen, T. Zhong, The study on the nonlinear computations of the DQ and DC methods, numerical methods for partial differential equations, Int. J. 13 (1) (1997) 57–75, https://doi.org/10.1002/(SICI)1098-2426(199701)13:1<57::AID-NUM5>3.0.CO;2-L.
[43] M. Şimşek, Nonlinear static and free vibration analysis of microbeams based on the nonlinear elastic foundation using modified couple stress theory and He's variational method, Compos. Struct. 112 (2014) 264–272, https://doi.org/10.1016/j.compstruct.2014.02.010.
[44] S. Sahmani, M. Bahrami, R. Ansari, Nonlinear free vibration analysis of functionally graded third-order shear deformable microbeams based on the modified strain gradient elasticity theory, Compos. Struct. 110 (2014) 219–230, https://doi.org/10.1016/j.compstruct.2013.12.004.
[45] A. Karamanli, Free vibration analysis of two directional functionally graded beams using a third order shear deformation theory, Compos. Struct. 189 (2018) 127–136, https://doi.org/10.1016/j.compstruct.2018.01.060.
[46] B. Karami, M. Janghorban, T. Rabczuk, Dynamics of two-dimensional functionally graded tapered Timoshenko nanobeam in thermal environment using nonlocal strain gradient theory, Compos. B Eng. 182 (2020), 107622, https://doi.org/10.1016/j.compositesb.2019.107622.
[47] M. Forghani, Y. Bazarganlari, P. Zahedinejad, MJ. Kazemzadeh-Parsi, Nonlinear frequency behavior of cracked functionally graded porous beams resting on elastic foundation using Reddy shear deformation theory, Jour. of Vib. and Cont. 29 (2023) 2454–2472, https://doi.org/10.1177/10775463221080213.